Scar-less whole-body regeneration in the absence of a blastema requires cell division in the ctenophore *Mnemiopsis leidyi*

Authors:

Julia Ramon Mateu[1], Mark Q. Martindale[1*]

Affiliation:

[1]The Whitney Laboratory for Marine Bioscience, 9505 N, Ocean Shore Blvd, St. Augustine, FL 32080-8610, USA

*Corresponding author

Email: mqmartin@whitney.ufl.edu

ABSTRACT

Most species of ctenophore (or “comb jelly”) possess an outstanding capacity to regenerate but the cellular and molecular mechanisms underlying this ability are unknown. We have studied wound healing and adult regeneration in the ctenophore *Mnemiopsis leidyi* and show that cell proliferation is activated at the wound site and is indispensable for whole-body regeneration. Wound healing occurs normally in the absence of cell proliferation forming a scar-less wound epithelium. No blastema is generated, rather undifferentiated cells assume the correct location of missing structures and differentiate in place. Cells originated in the main regions of cell proliferation do not seem to contribute to the formation of new structures suggesting a local source of cells during regeneration. Surprisingly, the ability to regenerate is recovered when exposure to cell-proliferation blocking treatment ends, suggesting that regenerative ability is constantly ready to be triggered and it is somehow independent of the wound healing process.

INTRODUCTION

Regeneration, the ability to re-form a body part that has been lost, is a widely shared property of metazoans (Bely and Nyberg, 2010). However, the contribution of cell proliferation, the source of regenerating tissue, and the mechanisms which pattern the replaced tissues varies greatly among animals with regenerative ability, resulting in a collection of different "modes" of regeneration (Alvarado and Tsonis, 2006; Tanaka and Reddien, 2011). The first classification of regenerative strategies was established by T. H. Morgan who initially defined two different mechanisms of rebuilding structures according to the contribution of cell proliferation: 1) *morphallaxis*, regeneration which occurs in the absence of active cell proliferation, through re-patterning of pre-existing tissue, and 2) *epimorphosis*, regeneration mediated by cell proliferation (Morgan, 1901). Epimorphic regeneration can involve the production of a blastema, a mass of undifferenciated cells that forms at the wound site from where cells proliferate and differentiate to form the missing structures (Sánchez Alvarado, 2000). The classical example of morphallactic regeneration is provided by the freshwater cnidarian polyp *Hydra*, which is able to regenerate the head after decapitation without a significant contribution from cell proliferation (Park et al., 1970; Cummings and Bode, 1984; Dübel and Schaller, 1990; Holstein et al., 1991; Chera et al., 2009). While documented cases of strict morphallaxis are very few in nature, most of the organisms with regenerative potential rely on cell proliferation (epimorphosis) – or a combination of both epimorphosis and morphallaxis – to re-form lost structures. Regenerative abilities appear to be diverse even within individual evolutionary clades. For example, regeneration of oral structures in another member of the phylum Cnidaria – *Nematostella vectensis* – is characterized by high levels of cell proliferation differing thus from the morphallactic regeneration potential in *Hydra* (Passamaneck and Martindale, 2012). In planarians, whole-body regeneration is accomplished by the proliferation of pluripotent stem cells (neoblasts), the only cells in the adult with proliferative potential, which form a mass of undifferentiated cells known as the regenerating blastema (Baguna et al., 1989; Newmark and Sánchez Alvarado, 2000; Wagner et al., 2011). Annelid regeneration provides examples of both epimorphic (blastema-based) regeneration and morphallactic (tissue-remodeling based) regeneration (Bely, 2014; Özpolat and Bely, 2016), showing diversity within the Lophotrochozoa. Moreover, evidence of cell migration has been documented during regeneration of several annelid species such as the freshwater annelid *Pristina leidyi* (Zattara et al., 2016) and the marine annelid worm *Capitella teleta,* in which local (proliferating cells close to the wound site) and distant (stem cell migration) sources of cells contribute to the formation of the regenerating blastema (de Jong and Seaver, 2017). Evidence of cell migration during regeneration is also provided by the

hydrozoan *Hydractinia echinata* in which stem cells (i-cells) from a remote area migrate to the wound site and contribute in the formation of the blastema (Bradshaw et al., 2015). In vertebrates, regenerative potential is limited primarily to the structural or cellular level. Urodele amphibians are known for being the only vertebrate tetrapods that can regenerate amputated limbs as adults. Similar to the previous examples of epimorphic regeneration, they require cell proliferation and the formation of a blastema. However, the urodele blastema is not generated from or composed of cells of a single type, but consists of a heterogeneous collection of lineage-restricted progenitors (Kragl et al., 2009). Moreover, diversity in the source of regenerating tissue has been reported among urodeles, with myofiber dedifferentiation being an integral part of limb regeneration in the newt but not in axolotl, in which resident multipotent muscle stem cells provide the regeneration activity (Sandoval-Guzmán et al., 2014). Dedifferentiation has also been described in another species of vertebrates, zebrafish, which can regenerate both heart and bone via dedifferentiation of mature cardiomyocytes and osteoblasts respectively (Jopling et al., 2010; Knopf et al., 2011).

Among the animals with impressive whole-body regenerative capabilities are lobate ctenophores (comb jellies), fragile holopelagic marine carnivores that represent one of the oldest extant metazoan lineages. Ctenophora is latin for “comb bearer”, referring to eight longitudinally oriented rows of locomotory ctene (or comb) plates which they coordinately beat to propel through the water column. Ctenphores possess a highly unique body plan characterized by a biradial symmetry (with no planes of mirror symmetry) and two epithelial layers: the ectoderm and the endoderm, separated by a thick mesoglea mostly composed of extracellular matrix, but also containing several types of individual muscle and mesenchymal cells. The oral-aboral axis is their major body axis and it is characterized by the mouth at one (oral) pole and the apical sensory organ at the opposite (aboral) pole. Most ctenophores possess a pair of muscular tentacles that bear specialized adhesive cells called colloblasts, used to capture prey (Pang and Martindale, 2008) (**Figure 1C**). One of the best studied species of ctenophores is the lobate ctenophore *Mnemiopsis leidyi,* which is emerging as a new model system in evolutionary-developmental biology (Henry and Martindale, 2000; Fischer et al., 2014; Schnitzler et al., 2014; Jager and Manuel, 2016; Reitzel et al., 2016; Martindale, 2016). *M. leidyi*’s life cycle is characterized by a rapid development including a highly stereotyped cleavage program and two adult stages: the juvenile tentaculate cydippid, distinguishable for having a pair of long branching tentacles (**Figure 1A,B**), and the lobate adult form which possess two oral feeding lobes. A particular feature of ctenophore embryogenesis is that they undergo mosaic development, meaning that embryos cannot compensate for cells/structures derived from cells killed or isolated

during early development. If blastomeres are separated at the two-cell stage, each will generate a "half-animal," possessing exactly half of the normal set of adult features (Freeman, 1967; Martindale, 1986). This lack of ability to replace missing parts during embryogenesis contrasts with the outstanding capacity to regenerate as adults. Both the tentaculate larval and lobate adult life stages of *M. leidyi* readily regenerate and are capable of whole-body regeneration from only a body quadrant or half (Martindale, 1986).

It has been known for well over 80 years that ctenophores have the capacity to replace missing body parts (Coonfield, 1936; Martindale, 1986; Martindale and Henry, 1996; Henry and Martindale, 2000; Tamm, 2012) but the cellular and molecular mechanisms underlying this ability are poorly understood. Is cell proliferation required for ctenophore regeneration? Is any kind of blastema-like structure formed during regeneration? What is the source and nature of cells that contribute to the regenerated structures? What is the role of the wound epidermis in regulating the future regenerative outcome? We have studied wound healing and adult regeneration in the ctenophore *Mnemiopsis leidyi* and show that cell proliferation is activated at the wound site several hours after wound healing is complete and is indispensable for the regeneration of all the structures of the cydippid's body. Wound healing occurs normally in the absence of cell proliferation forming a scar-less wound epithelium only a few hours after amputation. In both animals cut in half along the oral-aboral axis and those in which the apical organ is removed, anlage of all missing structures occurs within 48 hours and complete replacement of all cell types by 72 hours after the injury. No blastema is generated, rather undifferentiated cells assume the correct location of missing structures and differentiate in place. EdU (5-ethynyl-2'-deoxyuridine) labeling shows that in uncut animals the majority of cell divisions occur in the tentacle bulbs where the tentacles are continuously growing. In surgically challenged animals, cell division is stimulated at the wound site between 6-12 hours after injury and continues until 72 hours after injury. EdU pulse and chase experiments after surgery together with the removal of the two main regions of active cell proliferation suggest a local source of cells in the formation of missing structures. The appearance of new structures is completely dependent on cell division, however, surprisingly, the ability to regenerate is recovered when exposure to cell-proliferation blocking treatment ends, suggesting that the onset of regeneration is constantly ready to be triggered and it is somehow independent of the wound healing process. This study provides some first-time insights of the cellular mechanisms involved in ctenophore regeneration and paves the way for future molecular studies that will contribute to the understanding of the evolution of the regenerative ability throughout the animal kingdom.

RESULTS

Whole-body regeneration in *Mnemiopsis leidyi* cydippids

Although the regenerative response has been studied previously in *M. leidyi* (Coonfield, 1936; Martindale, 1986; Martindale and Henry, 1996; Henry and Martindale, 2000; Tamm, 2012) we first characterized the sequence of morphogenic events during cydippid wound healing and regeneration to provide a baseline for further experimental investigations. For this, two types of surgeries – representing the replacement of all the structures and cell types of the cydippid's body (e.g. apical organ, comb rows, tentacle bulbs and tentacles) – were performed (**Figure 1D**). The timing and order of formation of missing structures was assessed by *in vivo* imaging of the regenerating animals at different time points along the regeneration process.

Wound healing

To assess the mechanism of wound healing, juvenile cydippids were punctured generating a small epithelial gap (**Figure 2A**) (Imaging of larger wound healing events provided to be too difficult to document visually). Within minutes after puncture, the edges of the gap increased their thickness indicating the start of the wound closure. The next phase of wound closure was characterized by the migration of a small number of cells coming from deep levels of the mesoglea (underneath the epithelial layer) to the edges of the wound (**Figure 2B, Supplementary Figure 1**). Interestingly, while the migration of cells from the mesoglea to the wound site was quite evident, the migration of epithelial cells across the wounded area was not observed. Once the migrating deep cells adhered to the gap edges, they started to extend filopodia laterally towards the adjacent cells. The diameter of the gap was progressively reduced as the connections between filopodia of marginal cells pulled the edges of the wound together (**Figure 2C**). When the diameter of the gap was significantly reduced, the cells at the gap margins started to extend filopodia not only to adjacent cells but also to cells from the opposite edge of the wound. At this stage, multiple filopodia were detected emerging from a single cell (**Figure 2D**). Filopodia from all the edges of the wound eventually met forming a network of filaments that sealed the gap (**Figure 2E**) resulting in a scar-free epithelium within approximately 1.5-2 hours after the puncture.

Events during whole-body regeneration of the Mnemiopsis leidyi cydippid following bisection through the oral-aboral axis

Cydippids were bisected through the oral-aboral axis retaining the whole apical organ in one of the halves – bisected cydippids with a complete intact apical organ regenerate into whole animals in a higher percentage of the cases compared to bisected animals

with half apical organ (Martindale, 1986). Bisected cydippids containing half of the set of structures present in intact cydippids (four comb rows and one tentacle) and a complete apical organ were left to regenerate in 1x filtered sea water (1x FSW) (n>100) at 22ºC. Wound closure was initiated rapidly after bisection with the edges of the wound forming a round circumference that continued to reduce in diameter until meeting and was completed within 2 hours after bisection (hab). No scar or trace of the original wound was evident after this time. About 16 hab, four ciliated furrows – which connect the apical organ with the comb rows – appeared on a surface epithelium at the aboral end of the cut site (**Figure 3B**). A large blastema or mass of undifferentiated cells did not appear at the cut site. Rather, accumulations of cells were detected forming the primordia of all four of the future comb rows in a deeper plane at the end of each ciliated furrow. By 24 hab, the first comb plates appeared, first in the two most external (closer to existing comb rows) comb rows and later in the two internal rows (**Figure 3C**). Comb plate formation did not follow a consistent pattern initially. The correct orientation of comb plates and coordination of their beating was accomplished after a number of comb plates were formed (**Figure 3D** surface, down), as has been described previously (Tamm, 2012). Within 40 hab, coordinated comb plates were beating in all four regenerating comb rows and the primordia of tentacle bulb had emerged in the middle of the four comb rows. By 48 hab, regeneration of the missing structures of the cydippid body was essentially completed including the formation of the tentacle growing from the tentacle bulb (**Figure 3E**). At 96 hours after bisection, the regenerated tentacle was long enough to actively catch prey. The cut side continued to grow and within a day or two it was indistinguishable from the uncut side (**Figure 3F**).

Events during regeneration of the Mnemiopsis leidyi cydippid following apical organ amputation

Cydippids in which the apical organ was amputated were left to regenerate in 1x FSW (n>100) at 22ºC. The cut edges of the wound met and sealed within 30-60 minutes of the operation and the lesion was completely healed around 2 hours post amputation (hpa). Between 6 and 12 hpa, cells congregated under the wounded epithelium forming the primordia of the future apical organ (**Figure 4E-F'**). Extension of the ciliated furrows from each comb row towards the wound site could be spotted around 12 hpa. Within 24 hpa, cells at the wound site started to differentiate into the floor of the apical organ and its supporting cilia (**Figure 4G-H'**). At 48 hpa all the components of the statolith, including the supporting cilia, the balancing cilia and lithocytes, were formed (**Figure 4I-J'**). At approximately 60 hpa the complete set of structures forming the apical organ were regenerated with the exception of the polar fields (**Figure 4K-L'**). Within 3 days after

surgery, the polar fields had formed, and animals were indistinguishable from control animals of the same size.

Cell proliferation in intact cydippids

To identify areas of cell proliferation in juvenile *M. leidyi*, intact cydippids between 1.5 – 3.0 mm in diameter were labelled with the thymidine analog 5-ethynyl-20-deoxyuridine (EdU), which is incorporated into genomic DNA during the S-phase of the cell cycle (Salic and Mitchison, 2008; Chehrehasa et al., 2009; Alié et al., 2011; Schnitzler et al., 2014) (**Figure 5A**). Cydippids incubated with EdU during a 15-minute pulse showed a pattern of cell division characterized by two main regions of active cell proliferation corresponding to the two tentacle bulbs (**Figure 5B'**). Higher magnifications of these structures showed EdU staining specifically concentrated at the lateral and median ridges of the tentacle bulb. Two symmetrical populations of densely packed cells were observed at the aboral extremity of the lateral ridges, previously characterized by Alié et al. (2011) as the aboral/external cell masses (a.e.c.) (**Figure 5C'**). EdU labeling was also found in some cells of the apical organ and few isolated cells along the pharynx and under the comb rows (n=20, **Figure 5B-D'**). To detect dividing cells in M phase of the cell cycle we performed anti-phospho-histone 3 (anti-PH3) immunolabelings in intact cydippids. The spatial pattern and distribution of PH3 labeling closely matched the one described for EdU incorporation, although PH3+ cells were always about 10% less numerous than the EdU labeled cells, suggesting that the duration of the M phase is much shorter than the S phase (n=10, **Figure 5B'', C'', D''**).

In order to track the populations of proliferating cells over time in intact animals we performed EdU pulse-chase experiments consisting in a 15-minute EdU incubation (pulse) and a chase of different times followed by visualization (**Figure 5A**). After a 24h chase, the pools of proliferating cells had migrated from the tentacle bulb through the proximal region of the tentacles, although some EdU+ cells were still detected at the tentacle sheath. Increased labeling of nuclei in the apical organ, pharynx and comb rows was also observed (n=10, **Figure 5E-F'**). Following a 48h chase, the population of proliferating cells that was originally in the tentacle bulbs at the time of labeling had migrated to the most distal end of the tentacles, but only a few cells associated with the tentacle bulb showed long-term EdU retention, suggesting that there is a resident population of slowly dividing stem cells in the tentacle bulb as previously reported by Alié et al. (2011). The number of EdU+ nuclei along the pharynx, the apical sensory organ (specifically in the apical organ floor) and comb rows was considerably increased compared to the 24h chase condition (n=10, **Figure 5G-G')**, suggesting that there are either small populations of EdU labeled cells restricted to those areas that had

proliferated during the chase period, or that cells migrated in to those regions from regions of high mitotic density, or a combination of both events.

Cell proliferation is activated during ctenophore regeneration

Regeneration can be classified into two main categories according to the involvement of cell proliferation: epimorphosis, in which regeneration is mediated by active cell proliferation, and morphallaxis, in which regeneration can occur in the absence of cell proliferation, due to the remodeling of pre-existing cells (Sánchez Alvarado, 2000). In order to determine the role of cell proliferation in ctenophore regeneration we performed a series of EdU experiments in regenerating cydippids. A 15-minute exposure to EdU at different times after surgical cutting was evaluated after two types of surgeries that required different regenerative responses: a bisection through the oral-aboral axis and an apical organ ablation. The dynamics of cell proliferation at the wound site were quantified by calculating the ratio of EdU+ nuclei to total nuclei at different time-points following surgery (**Figure 6B** and **Figure 7B**).

Following oral-aboral bisection, EdU+ nuclei were first detected at the wound site between 6 and 12 hours after bisection (hab). There was some variability in the presence of EdU+ nuclei at 6 hab – with some specimens having fewer EdU+ nuclei at the wound site than others – however the presence of EdU+ cells was consistent in all the analyzed individuals by 12 hab. The few EdU+ cells at the early stages were scattered all along the cut site, but no aggregation of cells was observed (n=7, **Figure 6C-C''**). The number of EdU+ nuclei at the wound site slightly increased between 12 and 24 hab reaching a maximum at 24hab (**Figure 6B**), when EdU+ cells appeared concentrated in discrete areas forming the primordia of the regenerating tissues (the tentacle bulb and comb rows) (n=27, **Figure 6D-D''**). By 48 hab, the % of EdU+ nuclei had decreased as the cells started to differentiate into the final structures. EdU+ nuclei appeared confined into the regenerating comb rows and tentacle bulb, already distinguishable by nuclei staining (n=12, **Figure 6E-E''**). At 72 hab, the number of EdU+ nuclei at the comb rows was considerably reduced and these were concentrated at the oral end of the regenerating structures, where oral portions of structures are generated prior to aboral regions. For example, proliferative cells were no longer detected at the aboral end of the comb rows where cells had already differentiated into comb plates. In contrast, EdU+ cells at the regenerating tentacle bulb were abundant but appeared organized at the aboral extremity forming the two symmetrical populations of cells characteristic of the structure of the tentacle bulb (n=15, **Figure 6F-F'**). By 96 hab, when major repatterning events of regeneration were completed, EdU+ cells were only detected at the regenerated tentacle sheath forming the pattern of cell proliferation previously described in the tentacle bulbs

of intact cydippids (**Figure 4**) (n=5, **Supplementary figure 3A-A''**). In combination with EdU incorporation experiments, anti-PH3 immunostaining was performed at selected time-points following bisection. PH3+ cells were detected in the regenerating comb rows and tentacle bulb at 24 hab and 48 hab (**Supplementary figure 4A-B''**) consistent with the EdU incorporation, although the number of PH3+ cells was always less numerous than the EdU+ cells.

EdU labeling was also detected at the wound site of regenerating cydippids after apical organ amputation. Consistent with the oral-aboral bisection surgeries, EdU+ cells were first detected at 12 hpa suggesting that the start of the cell proliferation response occurred between the 6 and 12 hpa time points. A peak of cell proliferation was also observed at 24 hpa (**Figure 7B**), with EdU+ cells localized at the primordia of the apical organ, specifically in the apical organ floor and in the surrounding tissue including the regenerating comb rows adjacent to the cut site (n=15, **Figure 7E-F''**). The number of proliferating cells slightly decreased at 48 hpa when EdU+ cells were concentrated in the regenerating apical organ and were no longer found in the tissues near the wound site (n=20, **Figure 7G-H''**). By 72 hpa, the EdU+ nuclei were scarce and localized mostly along the polar fields in some specimens, while EdU+ nuclei were completely absent in other individuals at the same time-point (n=6, **Supplementary figure 3B-C''**). Anti-PH3 immunostaining showed presence of M-phase cells at the regenerating area at both 24 hpa and 48 hpa. Similar to half body regeneration, while only very few cells were labeled with anti-PH3, the pattern was consistent with the EdU labeling being the PH3+ cells more numerous at 24 hpa than 48 hpa (**Supplementary figure 4C-D'**).

Interestingly, for both types of surgeries, proliferating cells were not organized in a compacted mass of "blastema-like" cells from were new tissue formed. In contrast, proliferating cells were very few and scattered throughout the wound site at early time-points after surgery – when a blastema is normally formed in animals with epimorphic regeneration – and appeared more abundant and directly confined at the correct location of missing structures at later stages of regeneration, where they differentiated in place.

Cells participating in the regenerative response appear to arise locally

To investigate the source of cells that contribute to the formation of new tissue during ctenophore regeneration we performed a series of EdU pulse and chase experiments in regenerating cydippids. This technique has been successfully used in different model systems as a strategy to indirectly track populations of proliferating cells and determine its contribution to the formation of new structures (de Jong and Seaver, 2017; Planques et al., 2019). With the aim of determining whether cells proliferating before amputation contribute to the formation of new tissues, uncut cydippids were incubated in EdU, which

was incorporated into cells undergoing the S-phase of cell cycle. After a 15-minute pulse, EdU incorporation was blocked with several washes of thymidine and 1x FSW. Following the washes, apical organ amputations and oral-aboral bisections were performed and animals were left to regenerate in 1x FSW. The location of EdU+ cells was subsequently visualized at 24 and 48 hours after injury. In combination to EdU detection, an immunostaining against PH3 was performed in order to detect cells that were actively dividing in the animal immediately before fixation (**Figure 8A**).

No EdU+ cells were detected at the wound site at 24h (n=30) nor 48h (n=10) after bisection (**Figure 8B-C''**). EdU labeling at the tentacle bulb resembling the pattern of cells migrating from the tentacle bulb along the tentacle previously described (**Figure 5F-F'**) confirmed that the chase worked properly (**Figure 8B**). Moreover, presence of PH3+ cells were observed at the regenerating area indicating active cell division at the moment of fixation (**Figure 8B'' and 8C''**). Following apical organ amputation, few EdU+ nuclei were detected at the area of apical organ regeneration although the EdU signal was very weak, suggesting that these cells were the result of multiple rounds of division (n=13, **Figure 8D-D''**). After a 48h chase, few bright EdU+ nuclei were detected at the apical organ suggesting that S-phase cells from the uncut tissue might contribute to the formation of the apical sensory organ at later stages of regeneration (n=12, **Figure 8E-E''**). Presence of PH3+ cells at the regenerating apical organ confirmed active cell division at the apical organ area (**Figure 8E'-E''**). Taken together, these results show a minor contribution of proliferative cells originating in distant pre-existing proliferative tissue such as the tentacle bulbs to the formation of new structures.

Expression patterns determined through *in-situ* hybridization have reveled spatially restricted expression of the stem cell gene markers *Piwi, Vasa, Nanos and Sox* within areas of cell proliferation including the tentacle bulbs, in both juvenile cydippid and adult stages (Alié et al., 2011; Reitzel et al., 2016; Schnitzler et al., 2014). On the other hand, the ctenophore group of Beroids do not possess tentacles at any stage of their life cycle and they are the only group of ctenophores that have lost the ability to regenerate (Martindale, 2016). Based on these observations, it was hypothesized a role of tentacle bulbs as putative "stem cell niches" source of new cells during regeneration. To test this hypothesis, we physically removed both tentacle bulbs of juvenile cydippids and assessed they ability to regenerate. Two days after amputation all animals had regenerated all the cell types of the tentacle bulb (n>100, **Figure 9A-C'**). EdU labeling at different time-points after amputation showed activation of cell proliferation during tentacle bulb regeneration, consistent with the other two types of surgeries analyzed. EdU+ nuclei were first detected at the distal end of the endodermal canals at 18 hpa (n=10, **Figure 9E-E''**). At 24 hpa the number of EdU+ cells had increased, and they were

mainly organized forming the primordia of tentacle bulbs although some EdU+ cells were still detected at the tip of the endodermal canal connecting to the tentacle bulbs in formation (n=20, **Figure 9F-F''**). By 48 hpa, EdU+ nuclei appeared organized in the characteristic pattern of intact tentacle bulbs (**Figure 5B'** and **5C'**), and they were not detected at the endodermal canals any more (n=20, **Figure 9G-G''**). In addition, animals in which both tentacle bulbs and apical organ were removed, were able to regenerate all the missing structures (data not shown). These data argue strongly that the tentacle bulbs are not the source of multipotent stem cells required for the successful regenerative response in tentaculate ctenophores and point to a local source of cells in the formation of new structures.

Cell proliferation is strictly required for ctenophore regeneration

Having demonstrated that cell proliferation is activated during ctenophore regeneration, our next aim was to address the requirement of cell proliferation in the process of regeneration. Juvenile cydippids were exposed to hydroxyurea (HU) treatments, a drug that inhibits cell proliferation by blocking the ribonucleotide reductase enzyme and thereby preventing the S-phase of cell cycle (Young and Hodas, 1964). We first performed a dose-response test experiment in order to set the working concentration of HU in which animals could be continuously incubated during the complete period of regeneration with no significant disruption of their fitness. Concentrations of 20, 10 and 5mM HU were tested over a 72-hour time course. Incubations in 20 and 10mM HU were toxic and caused the degeneration and eventually death of most of the animals during the first 24 hours of incubation (data not shown). Incubations in 5mM HU were much less harmful; cydippids maintained a good condition swimming normally with no cell death over the 72-hour time course. We therefore decided to set 5mM HU as the working concentration for the cell proliferation inhibitor experiments. We then assessed the efficacy of that drug concentration in blocking cell proliferation in intact cydippids. Intact cydippids were incubated in 5mM HU for 24 and 72 hours and then incubated for 15 minutes with EdU as previously described (**Supplementary figure 6A**). At 24 hours of HU incubation, there was no detectable incorporation of EdU as compared with control cydippids, which showed the characteristic pattern of cell proliferation described in **Figure 5** (**Supplementary figure 6B-C'**). Inhibition of cell proliferation was maintained 72 hours after continuous HU incubation, as shown by the total absence of EdU+ cells in treated cydippids (**Supplementary figure 6D-E'**). Finally, we evaluated the effect of the drug during regeneration in dissected cydippids. Cydippids bisected through the aboral-oral axis and cydippids in which apical organ was amputated were exposed to a continuous incubation of 5mM HU from 0 to 72 hours after surgery. None of the bisected

cydippids had regenerated at 72 hours following HU treatment (n=75, **Figure 10D-E'**). Wound closure and healing occurred normally as shown by the continuous epidermal layer covering the wound (**Figure 10E**), but no sign of formation of the missing structures (tentacle bulb and comb rows) was observed. Likewise, none of the apical organ amputated cydippids had regenerated any of the structures/cell types of the missing apical organ at 72 hours following HU treatment, although the wound had correctly healed (n=55, **Figure 10H-J'**). Although HU treated animals failed to regenerate any of their missing structures, an aggregation of cells could be observed at the wound site (**Figures 10E** and **10J'**). These accumulations of quite large round-shaped cells could correspond to undifferentiated cells ready to re-form the missing structures but not able to proceed due to the blocking of cell proliferation. Importantly, the absence of EdU incorporation in dissected cydippids treated with HU confirmed that cell proliferation was completely suppressed (**Supplementary figure 6I-J'**). From these observations we concluded that regeneration was impaired due to the absence of cell proliferation, therefore, cell proliferation is indispensable for ctenophore regeneration to proceed in a normal way.

Regenerative ability is recovered after HU treatment ends

Hydroxyurea has been shown to be reversible in cell culture following removal of the inhibitor (Adams and Lindsay, 1967) (**Figure 11A**). HU treatments on dissected cydippids showed that wound healing occurs normally without cell division. In order to determine whether regeneration could be initiated in HU treated animals we took dissected cydippids that had been exposed to HU over 48 hours, washed them in 1x filtered sea water (1x FSW) to remove the inhibitor, and then followed their development for 48 hours to check for any ability to regenerate missing cell types (**Figures 11B and 11E**). Surprisingly, 36 out of 94 bisected cydippids (38%) had regenerated all the missing structures (comb rows, tentacle bulb and tentacle) 48 hours after HU had been removed (**Figure 11D-D''**). 58 out of 94 bisected cydippids (62%) showed some signs of regeneration but ultimately remained as "half animals", suggesting that these animals were not healthy enough to complete the regeneration process (Bading et al., 2017). (Note that these animals were not fed during the treatment (2 days) or recovery period (2 additional days)). On the other hand, 100% of the cydippids in which the apical organ was surgically removed and had been treated with HU for 48 hours, regenerated all the normal cell types of the apical organ (n=51, **Figure 11H-I'**). Moreover, bisected cydippids in which HU was added 4 hab (n=25) – when wound healing is already completed – and 12 hab (n=25) – when cells at the wound site have already begun to cycle – fail to regenerate the missing structures (data not shown). Altogether, these results show that

ctenophore regeneration can be initiated over 48 hours after wound healing is complete, hence, wound healing and regeneration appear to be two relatively independent events which can take place separately in time.

DISCUSSION

In this study, we provide a detailed morphological and cellular characterization of wound healing and regeneration in the ctenophore *Mnemiopsis leidyi*. Wound closure is initiated immediately after injury, with the edges of the wound forming a round circumference that moves over the underlying mesoglea as it continues to reduce in diameter until they meet and forming a scar-less wound epithelium by 2 hours following injury. Two main mechanisms seem to be pivotal for ctenophore wound closure: active cell migration of cells from the mesoglea underneath the epithelium upwards to the edges of the wound; and dynamic extension of filopodia by the leading-edge epithelial cells in order to zipper the wound edges together. Cell migration and formation of actin-based cellular protrusions have been described during wound closure in multiple systems (Begnaud et al., 2016), however, slight differences in those mechanisms have been observed in ctenophore wound healing. First, cell migration takes place in a “deep to surface” direction instead of a lateral direction, suggesting that only specific cell-types from the mesoglea, such as mesenchymal cells, have the ability to migrate and contribute to gap closure. Second, wound-edge cells in ctenophores organize their cytoskeleton in spike-shaped filopodia rather than in plate-like extensions (lamellipodia), which happen to be the most common type of cellular protrusions among different model systems of wound healing, including the cnidarian Clytia (Kamran et al., 2017). Despite these minor differences, the fact that common mechanisms of wound closure are shared between early branching phyla like ctenophores and cnidarians and bilaterians (including vertebrates) proves the ancient origin of wound healing mechanisms as a strategy to maintain epithelium integrity. Wound healing in *M. leidyi* occurs through changes in cell behavior and occurs normally in the absence of cell proliferation. This observation is consistent with the majority of animal models of regeneration found in cnidarians (Singer, 1971; Passamaneck and Martindale, 2012; Bradshaw et al., 2015; Amiel et al., 2015; Kamran et al., 2017) as well as with the more phylogenetically distantly-related marine annelid worm *Platynereis dumerilii* (Planques et al., 2019). Following wound healing and prior to activation of cell proliferation in *M. leidyi*, there is remodeling of the tissue surrounding the wound and small numbers of round-shaped cells sparsely congregate at the wound site suggesting a reorganization of the tissue in order to prepare it for regeneration. Ctenophore regeneration, however, is strictly associated with epimorphic regeneration since none of the missing structures can be reformed in the absence of cell

476 proliferation as proved by cell proliferation blocking treatments. Indeed, a combination of
477 both epimorphosis and morphallaxis strategies has been previously described in the
478 regeneration of other animals including annelids (De Jong and Seaver, 2016; Özpolat
479 and Bely, 2016), although in those cases morphallaxis takes place simultaneously with
480 epimorphosis – or even subsequent to epimorphosis – and is involved in the regeneration
481 of a specific structures such as parapodia (Berril, 1931) or the gut (Zattara and Bely,
482 2011).

483 Cell proliferation in *M. leidyi* is first detected at the wound site between 6-12 hours
484 after surgery. The percentage of proliferating cells increases progressively during the
485 first 12 hours following injury and reaches a maximum around 24 hours when the
486 primordia of the missing structures are clearly delineated. Following this peak of cell
487 proliferation, the percentage of cells undergoing cell division (S-phase) decreases while
488 cells start to differentiate into their final structures. Comparing the kinetics of cell
489 proliferation during regeneration of *M. leidyi* with the anthozoan cnidarian *Nematostella*
490 *vectensis* (Passamaneck and Martindale, 2012), the percentage of dividing cells at the
491 wound site is lower and the peak of maximum cell proliferation occurs earlier in
492 ctenophore regeneration. In intact cydippids, cell proliferation is concentrated in two main
493 areas of the cydippid's body corresponding to the tentacle bulbs. Some actively cycling
494 cells are also found in the apical organ as well as few isolated dividing cells along the
495 pharynx and under the comb rows. These results are consistent with previous EdU
496 analysis performed in *M. leidyi* cydippids (Schnitzler et al., 2014; Reitzel et al., 2016) and
497 adult ctenophores of the species *Pleurobrachia pileus* (Alié et al., 2011) where EdU
498 labeling has been detected in the same spatially restricted populations identified as stem
499 cell pools, specialized in the production of particular cell types. Pulse-chase experiments
500 show migration of proliferating cells from the tentacle bulb through to the distal tips of the
501 tentacle while a small population of slowly-dividing cells remains in the tentacle bulb.
502 These observations fit with histological and cellular descriptions of the tentacle apparatus
503 (Alié et al., 2011; Borisenko and Ereskovsky, 2013) which identified different populations
504 of undifferentiated progenitors source of all cell types found in the tentacle tissue.

505 Interestingly, proliferating cells during regeneration do not organize to form a
506 single large blastema-like structure from which a field of cells proliferate and differentiate
507 to form the missing structures. Rather, small numbers of undifferentiated cells assume
508 the correct location of all missing structures simultaneously and differentiate in place.
509 Considering the early branching phylogenetic position of ctenophores in the tree of life
510 (Dunn et al., 2008; Ryan et al., 2013), the absence of blastema during ctenophore
511 regeneration questions whether the formation of a blastema – which so far appears to

512 have been reported in representatives of all phyla of regenerating animals (Sánchez
513 Alvarado, 2000) – is a conserved trait throughout the evolution of regeneration.
514 The strict requirement of cell proliferation and the absence of blastema formation
515 make ctenophore regeneration a case of non-blastemal epimorphic regeneration.
516 Although far less common than the blastemal based regeneration, isolated cases of non-
517 blastemal regeneration have been reported such as lens regeneration by
518 transdifferentiation in newts (Tsonis and Del Rio-Tsonis, 2004) or liver regeneration by
519 compensatory proliferation in humans (Michalopoulos and DeFrances, 1997). EdU
520 pulse-chase experiments after amputation show little to no contribution of cells
521 originating in the main regions of active cell proliferation, including the tentacle bulbs, to
522 the formation of missing structures. Moreover, the removal of these structures (tentacle
523 bulbs), which have been reported to be localized areas of expression of genes involved
524 in stem cell maintenance and regulation of cell fate (Alié et al., 2011; Schnitzler et al.,
525 2014; Reitzel et al., 2016) and thus proposed to act as stem cell niches for regeneration,
526 do not prevent regeneration. These observations argue against the contribution of
527 discreet stem cell pools that migrate to and give rise to the re-formation of lost structures,
528 suggesting that new structures are generated from a local source of cells that become
529 activated to give rise to missing structures/cell types.
530 It is however important to note that our experiments do not answer the question
531 of the origin of cells that give rise to new structures. One possibility is that wound healing
532 activates the dedifferentiation of cells at the wound site that are reprogrammed to give
533 rise to whatever the appropriate set of cell types are needed to reconstitute the missing
534 structures. The accumulation of large undifferentiated cells at the wound site during HU
535 treatment is at least consistent with this scenario. In contrast, wound healing could
536 activate a dormant population of slowly-dividing pluripotent stem cells located uniformly
537 around the body that could migrate to the wound site and drive the regeneration process
538 which could have escaped/avoided the short pulse of EdU incorporation and re-entered
539 the cell cycle as a consequence of injury. Nonetheless, combination of cell-lineage and
540 specific cell-deletion experiments in *M. leidyi* showed that comb plate regeneration
541 cannot occur when the entire complement of cell lineage comb plate progenitors are
542 killed during embryogenesis, suggesting that, at least for comb plate regeneration, a
543 semi-committed somatic stem cell population is set-aside during embryogenesis for
544 comb plate replacement (Martindale and Henry, 1996, 1999). These data are premature
545 and need to be extended to other cell types and later stages of the regenerative process,
546 however the stereotyped cell lineage seen in ctenophores provides exciting opportunities
547 to pursue the origins of stem cells in the regenerative process in living animals.

Overall, our data, together with evidences from previous studies in ctenophores, support the strategy of local dedifferentiation and proliferation of progenitor cells as the main source of new tissue for ctenophore regeneration (**Figure 12**). Gene expression data during the process of *M. leidyi* regeneration combined with cell tracing experiments will contribute to refine our model of the origin of cells during ctenophore regeneration. Molecular data during regeneration will also be very valuable for performing comparisons of gene expression profiles between *M. leidyi* development (Levin et al., 2016) and regeneration and thus determine whether the molecular basis of ctenophore regeneration is similar to that deployed during development.

It is quite accepted that cells that re-epithelialize the wound provide the signals necessary to initiate regeneration (Brockes and Kumar, 2008; Owlarn et al., 2017). In vertebrates, local thrombin activation is a signal for regeneration as shown by the study in which cultured newt myotubes returned to the cell cycle by the activity of a thrombin-generated ligand (Tanaka et al., 1999). On the other hand, cellular interactions also seem to be important for the initiation of the regenerative response. One such case is the dorsoventral interaction between the wounded tissues during wound healing in planarians which has been shown to play a key role in the formation of the blastema and, hence, initiation of regeneration (Kato et al., 1999). These observations suggest that wound healing and regeneration are two closely related processes which need to take place sequentially in time. Our results, however, show that ctenophore regeneration can be initiated over 48 hours after wound healing is completed, suggesting that regeneration can be initiated without direct signaling induced by the wounded epithelium. Regeneration of the missing structures is not initiated until the cell proliferation blocking treatment is removed. Hence, another case scenario is that the wound epithelium produces persistent signaling necessary for triggering regeneration at the time of wound healing, but the process cannot be initiated due to the blocking of cell proliferation. This is consistent with the proposed hypothesis for *Nematostella* that the key transition from wound healing to a state of regeneration is the activation of cell proliferation (DuBuc et al., 2014). Studying and comparing the molecular signaling involved in both ctenophore wound healing and regeneration will be very useful to get further insight into the relationship between these two processes.

In conclusion, this study provides a rigorous description of the morphological and cellular events during ctenophore regeneration and compares them with the regenerative strategies followed by other metazoans. The early branching phylogenetic position of ctenophores together with their rapid, highly stereotyped development and remarkable ability to regenerate make them a key system to gain a better understanding of the evolution of animal regeneration.

MATERIALS AND METHODS

Animal care

Regeneration experiments were performed on juvenile *Mnemiopsis leidyi* cydippid stages due to their small size and ease of visualization and because their power of regeneration is the same as adults (Martindale, 1986). *M. leidyi* cydippids were obtained from spawning adults collected from either the floating docks located around Flagler Beach area, FL. USA, or from the floating docks at the east end of the Bridge of Lions on Anastasia Island, St. Augustine, FL. USA. For spawning, freshly collected adults were kept in constant light for at least two consecutive nights and then individual animals transferred into 6" diameter glass culture dishes filled with 1x FSW and placed in total darkness. After approximately 3-4 hours in the dark at 22-24ºC, these self-fertile hermaphroditic animals had spawned and embryos were collected by pipetting them into a new dish of UV treated 1.0 micron filtered full strength seawater (1x FSW) using a transfer pipette. Embryos were raised at 22-24ºC for approximately 5-7 days and fed once a day with rotifers (*Brachionus plicatilis*, 160µm) (Reed Mariculture, Campbell, CA. USA).

Animal surgeries

Operations were done in 35 mm plastic petri dishes with 2 mm thick silicon-coated bottoms (SYLGARD–184, Dow Corning, Inc.) on cydippids 1.5-3.0 mm in diameter. Cydippids were transferred in to the operation dishes in 0.2 µm-filtered seawater and cut using hand pulled glass needles from Pyrex capillaries (Martindale, 1986). Three types of operations were performed: 1) Oral-aboral bisections, in which animals were cut longitudinally through the esophageal plane generating two "half-animals". The operations were performed such that one half retained an intact apical organ while the remaining half lacked the apical organ. Only the halves retaining the apical organ were studied here as these halves regenerate to normal animals in a high percentage of the cases (Martindale, 1986). 2) Apical organ amputations, involving the removal of the apical organ by cutting perpendicular to the oral-aboral axis above the level of the tentacle bulbs. 3) Tentacle bulb amputations, consisting in the removal of both tentacle bulbs (**Figure 1D**). Following surgery, halves containing the apical organ, amputated cydippids without apical organ and amputated cydippids without tentacle bulbs were returned to 35 mm plastic Petri dishes filled with 0.2 µm filtered 1x FSW for the desired length of time without feeding. All the regenerating experiments were performed at 22-24ºC.

To study the wound healing process, juvenile cydippids were punctured generating a round-shaped wound of approximately 200-400 µm of diameter. Animals

were placed in a small drop of water over a Rain-X (Inc.) treated microscope slide and punctures were performed by pinching the epithelium layer using a pair of sharp needles (World Precision Instruments, Sarasota, FL. USA, Cat#500341). After puncture, animals were checked for the presence of an epithelial gap with the edges of the wound forming a small circumference exposing the mesoglea, and then they were immediately mounted for live imaging (see below).

Tissue labeling and cell counts

Detection of cell proliferation by incorporation of EdU

To label proliferating cells, cydippids were fixed and processed for fluorescent detection of incorporated EdU using the Click-iT EdU labeling kit (Invitrogen by Thermo Fisher Scientific, Waltham, MA. USA, Cat #C10424), which incorporates EdU in cells that are undergoing the S phase of the cell cycle. Specifically, intact cydippids between 1.5-3.0 mm in diameter or bisected/amputated cydippids were incubated in EdU labeling solution (100 µM of EdU in 1x FSW) for 15 minutes. For pulse-chase experiments cydippids were incubated with 100 µM EdU in 1x FSW for 15 minutes, washed 3 times with 100 µM thymidine in 1x FSW, and maintained in increasing volumes of 1x FSW until fixation. Control or operated cydippids were embedded in 1.2% low melt agarose (25ºC melting temperature, USB, Inc Cat #32830) in a 35 mm plastic petri dish (Fisher, Inc. Cat #08757100A) and fixed in ice-cold 100mM HEPES pH 6.9; 0.05M EGTA; 5mM MgSO4; 200mM NaCl; 1x PBS; 3.7% Formaldehyde; 0.2% Glutaraldehyde; 0.2% Triton X-100; and 1x FSW (0.2 µm filtered) for 1 hour at room temperature with gentle rocking (Salinas-Saavedra and Martindale, 2018). Animals were then washed several times in PBS-0.02% Triton X-100, then one time in PBS-0.2% Triton X-100 for 20 min, and again several times in PBS-0.02% Triton X-100. The EdU detection reaction was performed according to manufacturer instructions using the Alexa-567 reaction kit. Following detection, cydippids were washed three times in PBS-0.02% Triton X-100, and subsequently all nuclei were counterstained with DAPI (Invitrogen, Carlsbad, CA. USA, Cat. #D1306) at 1.43 µM in 1x PBS for 2 hours. Cydippids were mounted in TDE mounting media (97% TDE: 970µl 2,2'-thiodiethanol (Sigma-Aldrich, St. Louis, MO. USA); 30µl PBS) for visualization. To quantify the percentage of EdU labeled cells at the wound site, Zeiss 710 confocal z-stack projections of operated cydippids were generated using Fiji software (Image J) and individual cells were digitally counted using Imaris, Inc. software (Bitplane, Switzerland). Only the area and z-stacks surrounding the wound site were used for the analysis. EdU+ cells and nuclei were counted separately in 5 to 10 specimens for each time-point. The number of EdU-positive nuclei were divided by the

total number of nuclei stained with DAPI generating a ratio corresponding to the % of EdU+ cells.

Immunofluorescence

Proliferating cells in M phase were detected using an antibody against phospho Histone 3 (PH3 – phospho S10). Control or operated cydippids were fixed as mentioned above. Fixed cydippids were washed several times in PBS-0.02% Triton X-100 (PBT 0.02%), then one time in PBS-0.2% Triton X-100 (PBT 0.2%) for 10 min, and again several times in PBT 0.02%. They were then blocked in 5% normal goat serum (NGS; diluted in PBT 0.2%) for 1 hour at room temperature with gentle rocking. After blocking, specimens were incubated in anti-phospho histone H3 antibody (ARG51679, Arigo Biolaboratories, Taiwan) diluted 1:150 in 5% NGS overnight at 4ºC. The day after, specimens were washed at least five times with PBS-0.2% Triton X-100. Secondary antibody (Alexa Fluor 488 goat anti-rabbit IgG (A-11008, Invitrogen, Carlsbad, CA. USA) was diluted 1:250 in 5% NGS and incubated over night at 4ºC with gentle rocking. After incubation, specimens were washed three times with PBT 0.02% and incubated with DAPI (0.1µg/µl in 1x PBS; Invitrogen, Carlsbad, CA. USA, Cat. #D1306) for 2 hours to allow nuclear visualization. Samples were then rinsed in 1x PBS and mounted in TDE mounting media (97%TDE: 970µl 2,2'-thiodiethanol (Sigma-Aldrich, St. Louis, MO. USA); 30µl PBS) for visualization.

Cell proliferation inhibitor treatment with Hydroxyurea (HU)

Cell proliferation was blocked using the ribonucleotide reductase inhibitor hydroxyurea (HU) (Sigma-Aldrich, St. Louis, MO. USA). Incubations with hydroxyurea were performed at a concentration of 5 mM in 1x FSW. Operated cydippids were exposed to continuous incubations of 5mM HU for 48-72 hours. HU solution was exchanged with freshly diluted inhibitor every 12 hours. For washing experiments, the effect of HU was reversed by removal and replacement of the drug with 1x FSW.

Imaging

In vivo differential interference contrast (DIC) images were captured using a Zeiss Axio Imager M2 coupled with an AxioCam (HRc) digital camera. Fluorescent confocal imaging was performed using a Zeiss LSM 710 confocal microscope (Zeiss, Gottingen, Germany) using either a 20x/0.8 NA dry objective or a 40x/1.3 NA oil immersion objective.

For time-lapse imaging of the wound healing process, punctured cydippids were mounted in a hydrophobic-treated slide under a cover slip with clay corners. A hydrogel concentration of 7.5% in seawater (O'Bryan et al., 2019) was placed around the animals

as a mounting media in order to immobilize them during live-imaging. DIC images were captured using a Zeiss Axio Imager M2 coupled with a Rolera EM-C2 camera (Surrey, BC. Canada). Stacks were taken every minute. Generation of Z-stack projections, time-lapse movies and image processing was performed using Fiji software (Schindelin et al., 2012).

ACKNOWLEDGEMENTS

We thank Thomas Angelini for providing the hydrogels used for immobilizing cydippids during live imaging and all the members of our lab for assistance and discussions.

COMPETING INTERESTS

The authors declare that no competing interests exist.

REFERENCES

Adams, R.L.P., Lindsay, J.., 1967. Hydroxyurea. Reversal of inhibition and use as a cell-synchronizing agent. J. Biol. Chem. 242, 1314–1317.

Alié, A., Leclère, L., Jager, M., Dayraud, C., Chang, P., Le Guyader, H., Quéinnec, E., Manuel, M., 2011. Somatic stem cells express Piwi and Vasa genes in an adult ctenophore: Ancient association of “germline genes” with stemness. Dev. Biol. 350, 183–197. https://doi.org/10.1016/j.ydbio.2010.10.019

Alvarado, A.S., Tsonis, P.A., 2006. Bridging the regeneration gap: Genetic insights from diverse animal models. Nat. Rev. Genet. 7, 873–884. https://doi.org/10.1038/nrg1923

Amiel, A.R., Johnston, H.T., Nedoncelle, K., Warner, J.F., Ferreira, S., Röttinger, E., 2015. Characterization of morphological and cellular events underlying oral regeneration in the sea anemone, Nematostella vectensis. Int. J. Mol. Sci. 16, 28449–28471. https://doi.org/10.3390/ijms161226100

Bading, K.T., Kaehlert, S., Chi, X., Jaspers, C., Martindale, M.Q., Javidpour, J., 2017. Food availability drives plastic self-repair response in a basal metazoan-case study on the ctenophore Mnemiopsis leidyi A. Agassiz. Sci. Rep. 7, 1–9. https://doi.org/10.1038/s41598-017-16346-w

Baguna, J., Salo, E., Auladell, C., 1989. Regeneration and pattern formation in planarians. III. that neoblasts are Regeneration and pattern formation in planarians. III. that neoblasts are totipotent stem cells and the cells totipotent stem cells and the cells. Development 107, 77–86.

Begnaud, S., Chen, T., Delacour, D., Mège, R.M., Ladoux, B., 2016. Mechanics of epithelial tissues during gap closure. Curr. Opin. Cell Biol. 42, 52–62.

https://doi.org/10.1016/j.ceb.2016.04.006

Bely, A.E., Nyberg, K.G., 2010. Evolution of animal regeneration: re-emergence of a field. Trends Ecol. Evol. 25, 161–170. https://doi.org/10.1016/j.tree.2009.08.005

Bely, A.E., 2014. Early events in annelid regeneration: a cellular perspective. Integr. Comp. Biol. 54, 688–699. https://doi.org/10.1093/icb/icu109

Berrill NJ, 1931. Regeneration in Sabella pavonina (Sav.) and other sabellid worms. J Exp Zool. 58:495-523.

Borisenko, I., Ereskovsky, A. V., 2013. Tentacular apparatus ultrastructure in the larva of Bolinopsis infundibulum (Lobata: Ctenophora). Acta Zool. https://doi.org/10.1111/j.1463-6395.2011.00542.x

Bradshaw, B., Thompson, K., Frank, U., 2015. Distinct mechanisms underlie oral vs aboral regeneration in the cnidarian hydractinia echinata. Elife 2015, 1–19. https://doi.org/10.7554/eLife.05506

Brockes, J.P., Kumar, A., 2008. Comparative Aspects of Animal Regeneration. Annu. Rev. Cell Dev. Biol. 24, 525–549. https://doi.org/10.1146/annurev.cellbio.24.110707.175336

Chehrehasa, F., Meedeniya, A.C.B., Dwyer, P., Abrahamsen, G., Mackay-Sim, A., 2009. EdU, a new thymidine analogue for labelling proliferating cells in the nervous system. J. Neurosci. Methods 177, 122–130. https://doi.org/10.1016/j.jneumeth.2008.10.006

Chera, S., Ghila, L., Dobretz, K., Wenger, Y., Bauer, C., Buzgariu, W., Martinou, J.C., Galliot, B., 2009. Apoptotic Cells Provide an Unexpected Source of Wnt3 Signaling to Drive Hydra Head Regeneration. Dev. Cell 17, 279–289. https://doi.org/10.1016/j.devcel.2009.07.014

Coonfield, B.R., 1936. Regeneration in Mnemiopsis Leidyl Agassiz. Biol. Bull. 71, 421–428.

Cummings, S.G., Bode, H.R., 1984. Head regeneration and polarity reversal in Hydra attenuata can occur in the absence of DNA synthesis. Wilhelm Roux's Arch. Dev. Biol. 194, 79–86. https://doi.org/10.1007/BF00848347

De Jong, D.M., Seaver, E.C., 2016. A Stable Thoracic Hox Code and Epimorphosis Characterize Posterior Regeneration in Capitella teleta. PLoS One 11. https://doi.org/10.1371/journal.pone.0149724

De Jong, D.M., Seaver, E.C., 2017. Investigation into the cellular origins of posterior regeneration in the annelid *Capitella teleta*. Regeneration 1–17. https://doi.org/10.1002/reg2.94

Dübel, S., Schaller, H.C., 1990. Terminal Differentiation of Ectodermal Epithelial Stem Cells of Hydra Can Occur in G2 without Requiring Mitosis or S Phase. J. Cell Biol.

110, 939–945. https://doi.org/10.1083/jcb.110.4.939

DuBuc, T.Q., Traylor-Knowles, N., Martindale, M.Q., 2014. Initiating a regenerative response; cellular and molecular features of wound healing in the cnidarian Nematostella vectensis. BMC Biol. 12, 1–20. https://doi.org/10.1186/1741-7007-12-24

Dunn, C.W., Hejnol, A., Matus, D.Q., Pang, K., Browne, W.E., Smith, S.A., Seaver, E., Rouse, G.W., Obst, M., Edgecombe, G.D., Sørensen, M. V., Haddock, S.H.D., Schmidt-Rhaesa, A., Okusu, A., Kristensen, R.M., Wheeler, W.C., Martindale, M.Q., Giribet, G., 2008. Broad phylogenomic sampling improves resolution of the animal tree of life. Nature 452, 745–749. https://doi.org/10.1038/nature06614

Fischer, A.H.L., Pang, K., Henry, J.Q., Martindale, M.Q., 2014. A cleavage clock regulates features of lineage-specific differentiation in the development of a basal branching metazoan, the ctenophore Mnemiopsis leidyi. Evodevo 5. https://doi.org/10.1186/2041-9139-5-4

Freeman, G., 1967. Studies on regeneration in the creeping ctenophore, Vallicula multiformis. J. Morphol. https://doi.org/10.1002/jmor.1051230107

Henry, J.Q., Martindale, M.Q., 2000. Regulation and regeneration in the ctenophore Mnemiopsis leidyi. Dev. Biol. 227, 720–733. https://doi.org/10.1006/dbio.2000.9903

Holstein, T.W., Hobmayer, E., David, C.N., 1991. Pattern of epithelial cell cycling in hydra. Dev. Biol. 148, 602–611. https://doi.org/10.1016/0012-1606(91)90277-A

Jager, M., Manuel, M., 2016. Ctenophores: an evolutionary-developmental perspective. Curr. Opin. Genet. Dev. 39, 85–92. https://doi.org/10.1016/j.gde.2016.05.020

Jopling, C., Sleep, E., Raya, M., Martí, M., Raya, A., Belmonte, J.C.I., 2010. Zebrafish heart regeneration occurs by cardiomyocyte dedifferentiation and proliferation. Nature 464, 606–609. https://doi.org/10.1038/nature08899

Kamran, Z., Zellner, K., Kyriazes, H., Kraus, C.M., Reynier, J.B., Malamy, J.E., 2017. In vivo imaging of epithelial wound healing in the cnidarian Clytia hemisphaerica demonstrates early evolution of purse string and cell crawling closure mechanisms. BMC Dev. Biol. 17, 1–14. https://doi.org/10.1186/s12861-017-0160-2

Kato, K., Orii, H., Watanabe, K., Agata, K., 1999. The role of dorsoventral interaction in the onset of planarian regeneration. Development 126, 1031–1040. https://doi.org/10.1242/dev.031682

Knopf, F., Hammond, C., Chekuru, A., Kurth, T., Hans, S., Weber, C.W., Mahatma, G., Fisher, S., Brand, M., Schulte-Merker, S., Weidinger, G., 2011. Bone regenerates via dedifferentiation of osteoblasts in the zebrafish fin. Dev. Cell 20, 713–724.

https://doi.org/10.1016/j.devcel.2011.04.014

Kragl, M., Knapp, D., Nacu, E., Khattak, S., Maden, M., Epperlein, H.H., Tanaka, E.M., 2009. Cells keep a memory of their tissue origin during axolotl limb regeneration. Nature 460, 60–65. https://doi.org/10.1038/nature08152

Levin, M., Anavy, L., Cole, A.G., Winter, E., Mostov, N., Khair, S., Senderovich, N., Kovalev, E., Silver, D.H., Feder, M., Fernandez-Valverde, S.L., Nakanishi, N., Simmons, D., Simakov, O., Larsson, T., Liu, S.-Y., Jerafi-Vider, A., Yaniv, K., Ryan, J.F., Martindale, M.Q., Rink, J.C., Arendt, D., Degnan, S.M., Degnan, B.M., Hashimshony, T., Yanai, I., 2016. The mid-developmental transition and the evolution of animal body plans. Nature 531, 637.

Martindale, M.Q., 1986. The ontogeny and maintenance of adult symmetry properties in the ctenophore, Mnemiopsis mccradyi. Dev. Biol. https://doi.org/10.1016/0012-1606(86)90026-6

Martindale, M.Q., 2016. The onset of regenerative properties in ctenophores. Curr. Opin. Genet. Dev. https://doi.org/10.1016/j.gde.2016.06.017

Martindale, M.Q., Henry, J.Q., 1996. Development and Regeneration of Comb Plates in the Ctenophore Mnemiopsis leidyi. Biol. Bull. 191, 290–292. https://doi.org/10.1086/BBLv191n2p290

Martindale, M.Q., Henry, J.Q., 1999. Intracellular Fate Mapping in a Basal Metazoan, the Ctenophore Mnemiopsis leidyi, Reveals the Origins of Mesoderm and the Existence of Indeterminate Cell Lineages. Dev. Biol. 214, 243–257.

Michalopoulos, G.K., DeFrances, M., 1997. Liver regeneration. Science (80-.). 276, 60–66. https://doi.org/10.1007/b99968

Morgan, T.H., 1901. Regeneration. New York: The Macmillan Company.

Newmark, P.A., Sánchez Alvarado, A., 2000. Bromodeoxyuridine specifically labels the regenerative stem cells of planarians. Dev. Biol. 220, 142–153. https://doi.org/10.1006/dbio.2000.9645

O'Bryan, C.S., Kabb, C.P., Sumerlin, B.S., Angelini, T.E., 2019. Jammed Polyelectrolyte Microgels for 3D Cell Culture Applications: Rheological Behavior with Added Salts. ACS Appl. Bio Mater. https://doi.org/10.1021/acsabm.8b00784

Owlarn, S., Klenner, F., Schmidt, D., Rabert, F., Tomasso, A., Reuter, H., Mulaw, M.A., Moritz, S., Gentile, L., Weidinger, G., Bartscherer, K., 2017. Generic wound signals initiate regeneration in missing-tissue contexts. Nat. Commun. 8, 1–13. https://doi.org/10.1038/s41467-017-02338-x

Özpolat, B.D., Bely, A.E., 2016. Developmental and molecular biology of annelid regeneration: a comparative review of recent studies. Curr. Opin. Genet. Dev. 40, 144–153. https://doi.org/10.1016/j.gde.2016.07.010

Pang, K., Martindale, M.Q., 2008. Comb jellies (Ctenophora): A model for basal metazoan evolution and development. Cold Spring Harb. Protoc. 3, 1–11. https://doi.org/10.1101/pdb.emo106

Park, H.D., Ortmeyer, A.B., Blankenbaker, D.P., 1970. Cell Division during Regeneration in Hydra. Nature 228, 227–231.

Passamaneck, Y.J., Martindale, M.Q., 2012. Cell proliferation is necessary for the regeneration of oral structures in the anthozoan cnidarian Nematostella vectensis. BMC Dev. Biol. 12. https://doi.org/10.1186/1471-213X-12-34

Planques, A., Malem, J., Parapar, J., Vervoort, M., Gazave, E., 2019. Morphological, cellular and molecular characterization of posterior regeneration in the marine annelid Platynereis dumerilii. Dev. Biol. 445, 189–210. https://doi.org/10.1016/j.ydbio.2018.11.004

Reitzel, A.M., Pang, K., Martindale, M.Q., 2016. Developmental expression of “germline”- and “sex determination”-related genes in the ctenophore Mnemiopsis leidyi. Evodevo 7, 1–16. https://doi.org/10.1186/s13227-016-0051-9

Ryan, J.F., Pang, K., Schnitzler, C.E., Nguyen, A.D., Moreland, R.T., Simmons, D.K., Koch, B.J., Francis, W.R., Havlak, P., Smith, S.A., Putnam, N.H., Haddock, S.H.D., Dunn, C.W., Wolfsberg, T.G., C.Mullikin, J., Martindale, M.Q., Baxevanis, A.D., 2013. The genome of the ctenophore Mnemiopsis leidyi and its implications for cell type evolution. Science (80-.). 342. https://doi.org/10.1126/science.1242592

Salic, A., Mitchison, T.J., 2008. A chemical method for fast and sensitive detection of DNA synthesis in vivo. PNAS 105. https://doi.org/10.1073/pnas.0712168105

Salinas-Saavedra, M., Martindale, M.Q., 2018. Improved protocol for spawning and immunostaining embryos and juvenile stages of the ctenophore _Mnemiopsis leidyi_.

Sánchez Alvarado, A., 2000. Regeneration in the metazoans: why does it happen? BioEssays 22, 578–590.

Sandoval-Guzmán, T., Wang, H., Khattak, S., Schuez, M., Roensch, K., Nacu, E., Tazaki, A., Joven, A., Tanaka, E.M., Simon, A., 2014. Fundamental differences in dedifferentiation and stem cell recruitment during skeletal muscle regeneration in two salamander species. Cell Stem Cell 14, 174–187. https://doi.org/10.1016/j.stem.2013.11.007

Schindelin, J., Arganda-Carreras, I., Frise, E., Kaynig, V., Longair, M., Pietzsch, T., Preibisch, S., Rueden, C., Saalfeld, S., Schmid, B., Tinevez, J.-Y., White, D.J., Hartenstein, V., Eliceiri, K., Tomancak, P., Cardona, A., 2012. Fiji: an open-source platform for biological-image analysis. Nat. Methods 9, 676–82.

880 https://doi.org/10.1038/nmeth.2019
881 Schnitzler, C.E., Simmons, D.K., Pang, K., Martindale, M.Q., Baxevanis, A.D., 2014.
882 Expression of multiple Sox genes through embryonic development in the
883 ctenophore Mnemiopsis leidyi is spatially restricted to zones of cell proliferation.
884 Evodevo 5, 1–17. https://doi.org/10.1186/2041-9139-5-15
885 Singer, I.I., 1971. Tentacular and oral-disc regeneration in the sea anemone, Aiptasia
886 diaphana. J. Embryol. Exp. Morphol. 26, 253–270.
887 https://doi.org/10.1007/BF00597293
888 Tamm, S.L., 2012. Regeneration of Ciliary Comb Plates in the Ctenophore Mnemiopsis
889 leidyi. I. Morphology. J. Morphol. 109–120. https://doi.org/10.1002/jmor.11016
890 Tanaka, E.M., Drechsel, D.N., Brockes, J.P., 1999. Thrombin regulates S-phase re-
891 entry by cultured newt myotubes. Curr. Biol. 9, 792–799.
892 https://doi.org/10.1016/S0960-9822(99)80362-5
893 Tanaka, E.M., Reddien, P.W., 2011. The Cellular Basis for Animal Regeneration. Dev.
894 Cell 21, 172–185. https://doi.org/10.1016/j.devcel.2011.06.016
895 Tsonis, P.A., Del Rio-Tsonis, K., 2004. Lens and retina regeneration:
896 Transdifferentiation, stem cells and clinical applications. Exp. Eye Res. 78, 161–
897 172. https://doi.org/10.1016/j.exer.2003.10.022
898 Wagner, D.E., Wang, I.E., Reddien, P.W., 2011. Clonogenic neoblasts are pluripotent
899 adult stem cells that underlie planarian regeneration. Science (80-.). 332, 811–
900 816. https://doi.org/10.1126/science.1203983.
901 Young CW, Hodaas S, 1964. Hydroxyurea: inhibitory effect on DNA metabolism.
902 Science. 146:1172–1174.
903 Zattara, E.E., Bely, A.E., 2011. Evolution of a novel developmental trajectory: Fission is
904 distinct from regeneration in the annelid Pristina leidyi. Evol. Dev. 13, 80–95.
905 https://doi.org/10.1111/j.1525-142X.2010.00458.x
906 Zattara, E.E., Turlington, K.W., Bely, A.E., 2016. Long-term time-lapse live imaging
907 reveals extensive cell migration during annelid regeneration. BMC Dev. Biol. 16,
908 1–21. https://doi.org/10.1186/s12861-016-0104-2
909

FIGURES AND LEGENDS

Figure 1

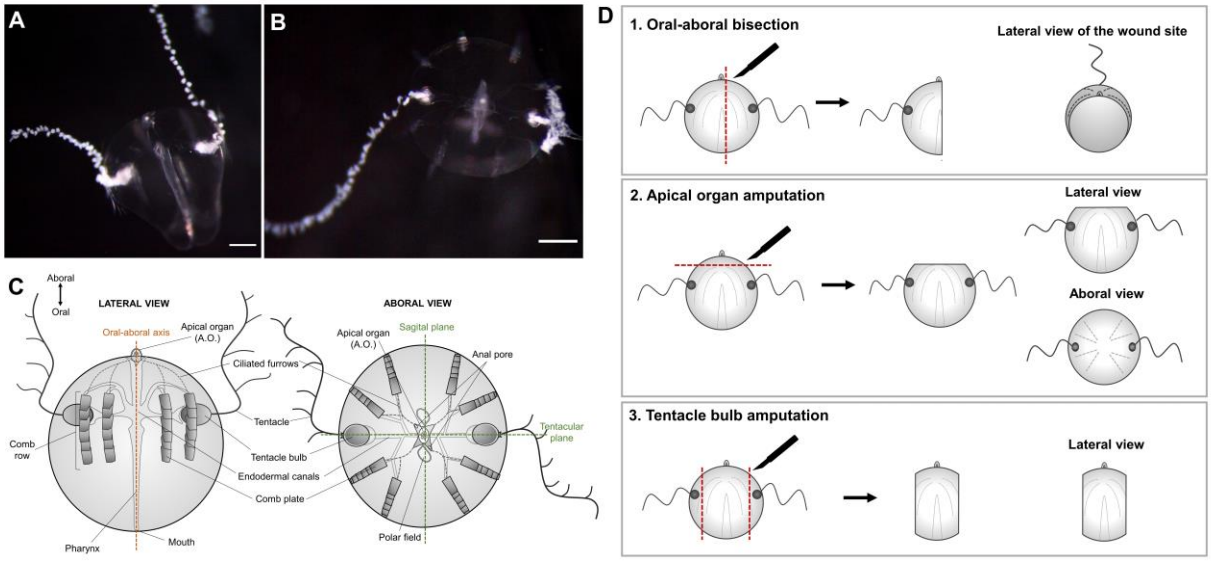

Figure 1. Cydippid stage of *Mnemiopsis leidyi* and animal surgeries. (**A**) Lateral view of a *M. leidyi* cydippid. (**B**) Aboral view of a *M.leidyi* cydippid. Scale bars = 100μm. (**C**) Schematic representation of the body plan of a cydippid stage in a lateral and aboral views. (**D**) Diagrams showing the three types of animal surgeries performed in this study and the views presented for each one.

Figure 2

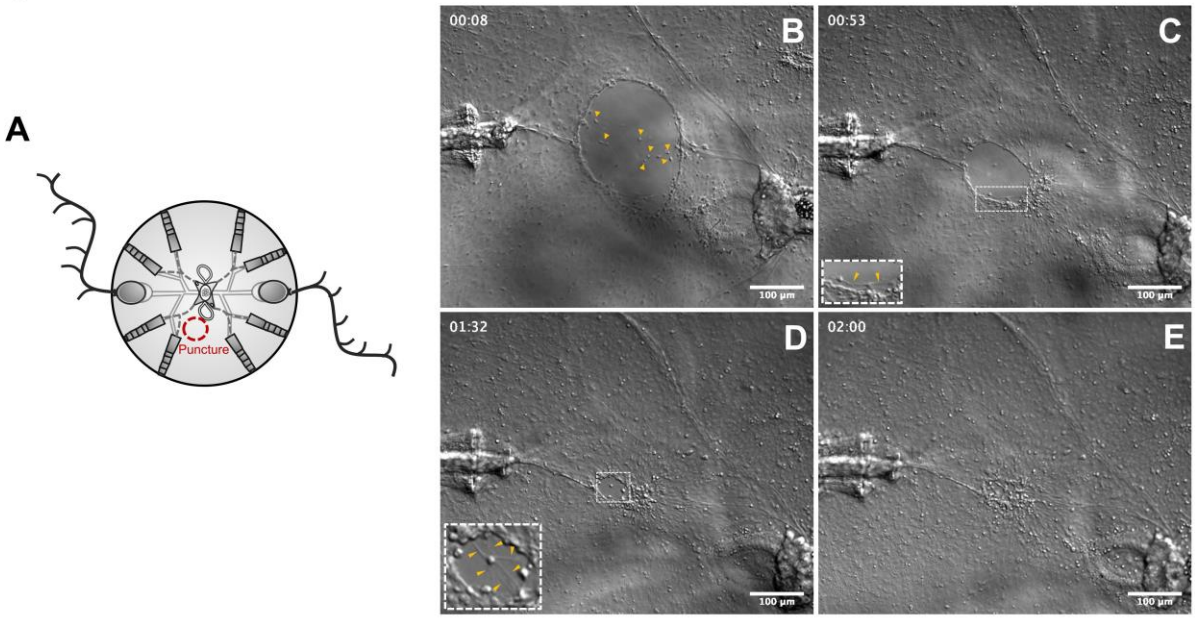

Figure 2. Wound healing by filopodia-dependent cell crawling. (**A**) Schematic representation of the puncture assay. (**B-E**) DIC images of the main phases of wound closure (See Supplementary file 2 for the time lapse video corresponding to these images). (**B**) Cells from the mesoglea (yellow arrow caps) migrate upwards and adhere to the edges of the wound. (**C**) Marginal cells of the wound gap extend filopodia to the adjacent cells pulling the edges of the wound together. The inset shows a closer look to the cells at the edge of the wound and yellow arrow caps point to the filopodia. (**D**) When the diameter of the gap is considerably reduced, cells of the wound edge extend filopodia towards the opposite edges of the gap. The inset shows a cell extending multiple filopodia. (**E**) Network of filopodia connecting all the edges of the wound. Scale bars = 100μm.

Figure 3

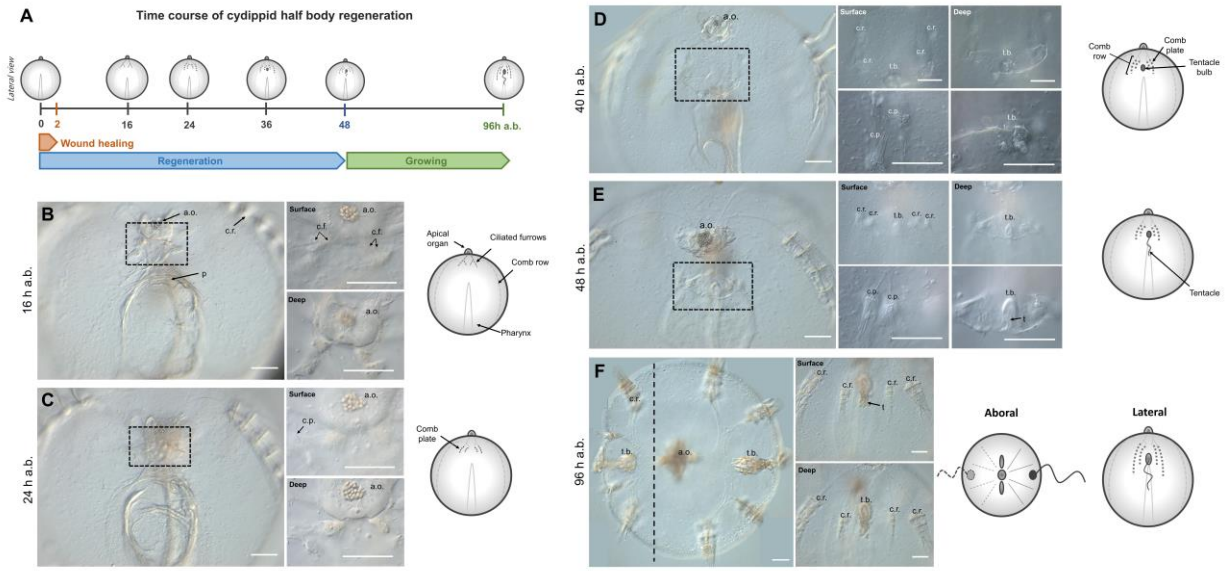

Figure 3. Half body regeneration in *Mnemiopsis leidyi* cydippid. (**A**) Schematic representation of the time course of morphogenic events during cydippid half body regeneration. All cartoons correspond to lateral views of the cydippid's body bisected through the oral-aboral axis showing the cut site in the first plane. The apical organ is located at the aboral end (top) and the mouth at the oral end (down). For simplicity, tissues on the opposite body site are not depicted. (**B-F**) DIC images showing the cut site of regenerating cydippids from 16 to 96 hab. Dotted line rectangles in (**B**), (**C**), (**D**) and (**E**) show the area corresponding to higher magnifications on the right. Magnifications show surface and deep planes. The vertical dotted line in (**F**) indicates the approximate position of bisection, and all tissue in the left of the line is regenerated tissue. Scale bars = 100 μm. Abbreviations: hours after bisection (h a.b.), apical organ (a.o.), pharynx (p), comb row (c.r.), ciliated furrow (c.f.), comb plate (c.p.), tentacle bulb (t.b.), tentacle (t).

Figure 4

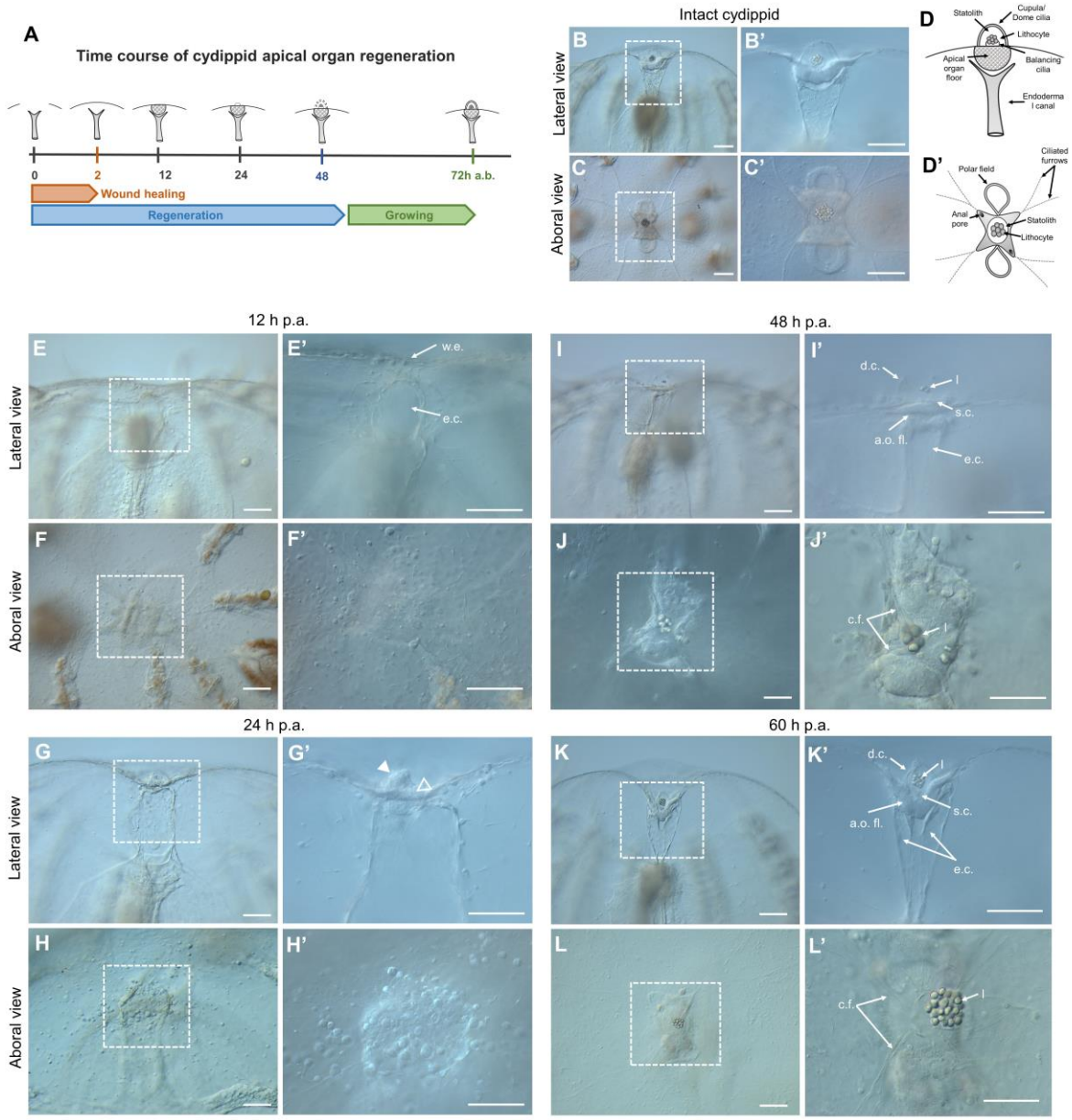

Figure 4. Apical organ regeneration in *Mnemiopsis leidyi* cydippids. (**A**) Schematic representation of the time course of morphogenic events during cydippid's apical organ regeneration. Cartoons correspond to lateral views of the apical sensory organ at different stages of regeneration. (**B-C'**) DIC images of the apical organ of an intact cydippid in lateral (**B-B'**) and aboral (**C-C'**) views. (**D-D**) Schematic of the components of the apical sensory organ in lateral (**D**) and aboral (**D'**) views. (**E-L'**) DIC images showing the cut site of regenerating cydippids after apical organ amputation from 12 to 60 hpa. Lateral and aboral views are included. Dotted line rectangles delimit the area corresponding to higher magnifications on the right. Filled and empty white arrow caps in (**G'**) point to aggregation of cells forming the primordia of the future statolith and apical organ floor respectively. Scale bars = 100 μm. Abbreviations: hours post amputation (h p.a.), wound epithelium (w.e.), endodermal canal (e.c.), dome cilia (d.c.), lithocyte (l), supporting cilia (s.c.), apical organ floor (a.o. fl.), ciliated furrows (c.f.).

Figure 5

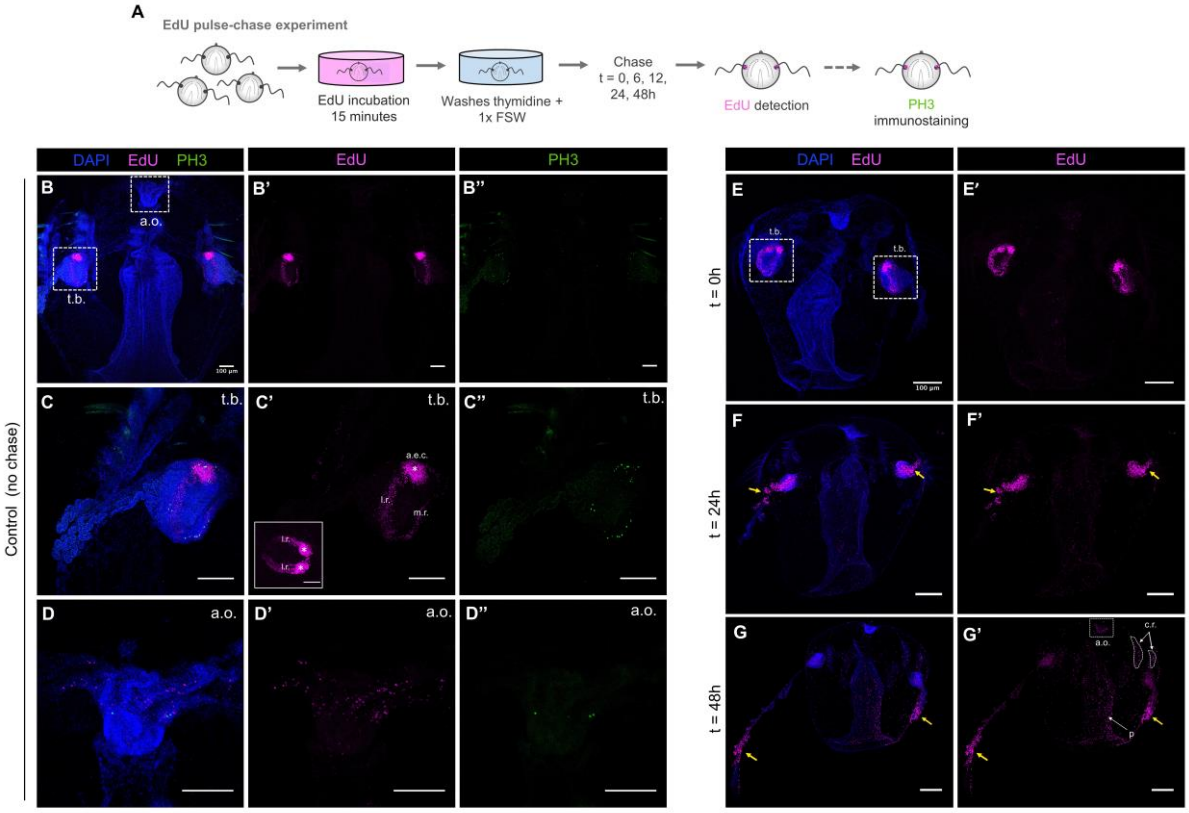

Figure 5. Cell proliferation in intact cydippids. (**A**) Schematic of the EdU pulse-chase experiment and PH3 immunostaining in intact cydippids. (**B-D'**) Confocal stack projections of whole intact cydippids oriented in a lateral view. White dotted rectangles in (**B)** delimit the tentacle bulb (t.b.) (**C-C'''**) and apical organ (a.o.) (**D-D'''**) structures showed in higher magnification at the bottom. Nuclei of S-phase cells are labeled with EdU (magenta), M-phase cells are immunostained with anti-phospho-Histone 3 (PH3) (green) and all nuclei are counterstained with DAPI (blue). Note that both markers of cell proliferation (EdU and PH3) show the same pattern of distribution along the cydippid's body. The inset in (**C'**) shows an aboral view of the tentacle bulb after EdU staining. White asterisks in (**C'**) point to the symmetrical populations of intense cell proliferation referred as aboral/external cell masses (a.e.c.). (**E-G'**) Confocal stack projections of whole intact cydippids oriented in a lateral view. The time of the chase is listed at the top of the columns, and the labeling corresponding to each panel is listed to the left of the rows. Nuclei of S-phase cells are labeled with EdU (magenta) and all nuclei are counterstained with DAPI (blue). Note that EdU+ cells migrate from the tentacle bulb to the most distal end of the tentacle (yellow arrows). See **Supplementary Figure 2** for further detail of EdU pulse-chase experiment in the tentacle bulb. Scale bars = 100 μm. Abbreviations: apical organ (a.o.), tentacle bulb (t.b.), aboral/external cell masses (a.e.c.), lateral ridge (l.r.), medial ridge (m.r.), comb row (c.r.).

Figure 6

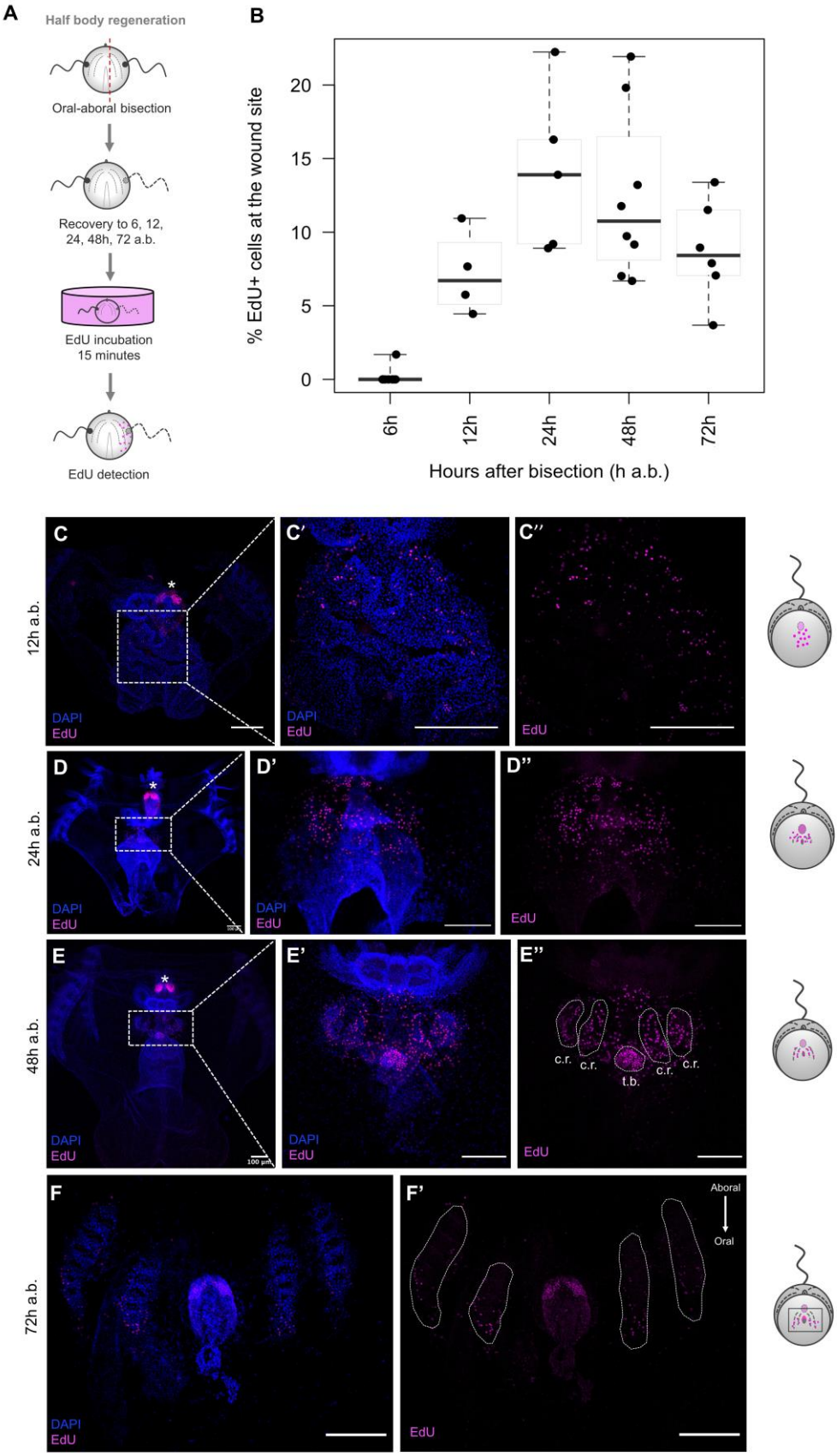

Figure 6. Cell proliferation during half body regeneration. (**A**) Schematic of the EdU incorporation experiment in cydippids bisected through the oral-aboral axis. (**B**) Box plot showing the levels of cell proliferation at the wound site at different time points after bisection. The thick horizontal bars indicate the median values. Each dot represents one individual. (**C-F'**) Confocal stack projections of bisected cydippids through the oral-aboral axis oriented in a lateral view showing the cut site in the first plane. The time following bisection is listed to the left of the rows. Nuclei of S-phase cells are labeled with EdU (magenta) and all nuclei are counterstained with DAPI (blue). The pattern of EdU labeling corresponding to each time-point is shown in a cartoon on the right of the rows. Dotted line rectangles in (**C**), (**D**) and (**E**) show the area corresponding to higher magnifications on the right. White dotted lines in (**E''**) and (**F'**) delimit the area corresponding to the regenerating comb rows and tentacle bulb. White asterisks point to tentacle bulbs of the uncut site. Note that EdU+ cells at 72 hpa (**F'**) are located at the oral end of the regenerating comb rows and no EdU+ cells are detected at the aboral end where cells are already differentiated. Scale bars = 100 μm. Abbreviations: hours after bisection (h a.b.) comb row (c.r.), tentacle bulb (t.b.).

Figure 7

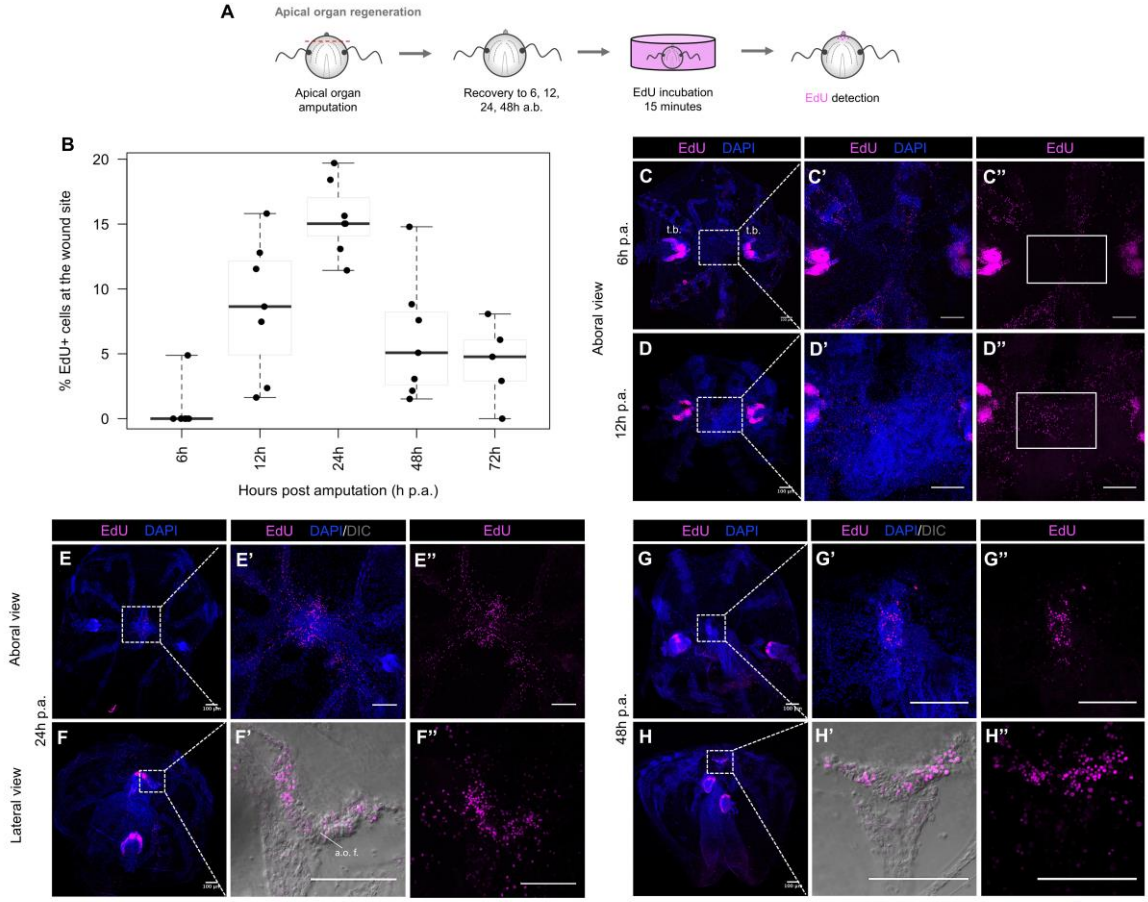

Figure 7. Cell proliferation during apical organ regeneration. (**A**) Schematic of the EdU incorporation experiment in cydippids in which the apical organ was amputated. (**B**) Box plot showing the levels of cell proliferation at the wound site at different time points post amputation. The thick horizontal bars indicate the median values. Each dot represents one individual. (**C-H''**) Confocal stack projections of cydippids in which the apical organ was amputated at different time points post amputation. Aboral and lateral views are shown. The labeling corresponding to each panel is listed at the top of the columns, and the time following amputation is listed to the left of the rows. Dotted line rectangles in (**C**), (**D**), (**E**), (**F**), (**G**) and (**H**) show the area corresponding to higher magnifications on the right. White rectangles in (**C''**) and (**D''**) delimit the area of apical organ regeneration. Nuclei of S-phase cells are labeled with EdU (magenta) and all nuclei are counterstained with DAPI (blue). DIC images of the tissue are shown in (**F'**) and (**H'**). Scale bars = 100 μm. Abbreviations: tentacle bulb (t.b.), apical organ floor (a.o. f), hours post amputation (h p.a.).

Figure 8

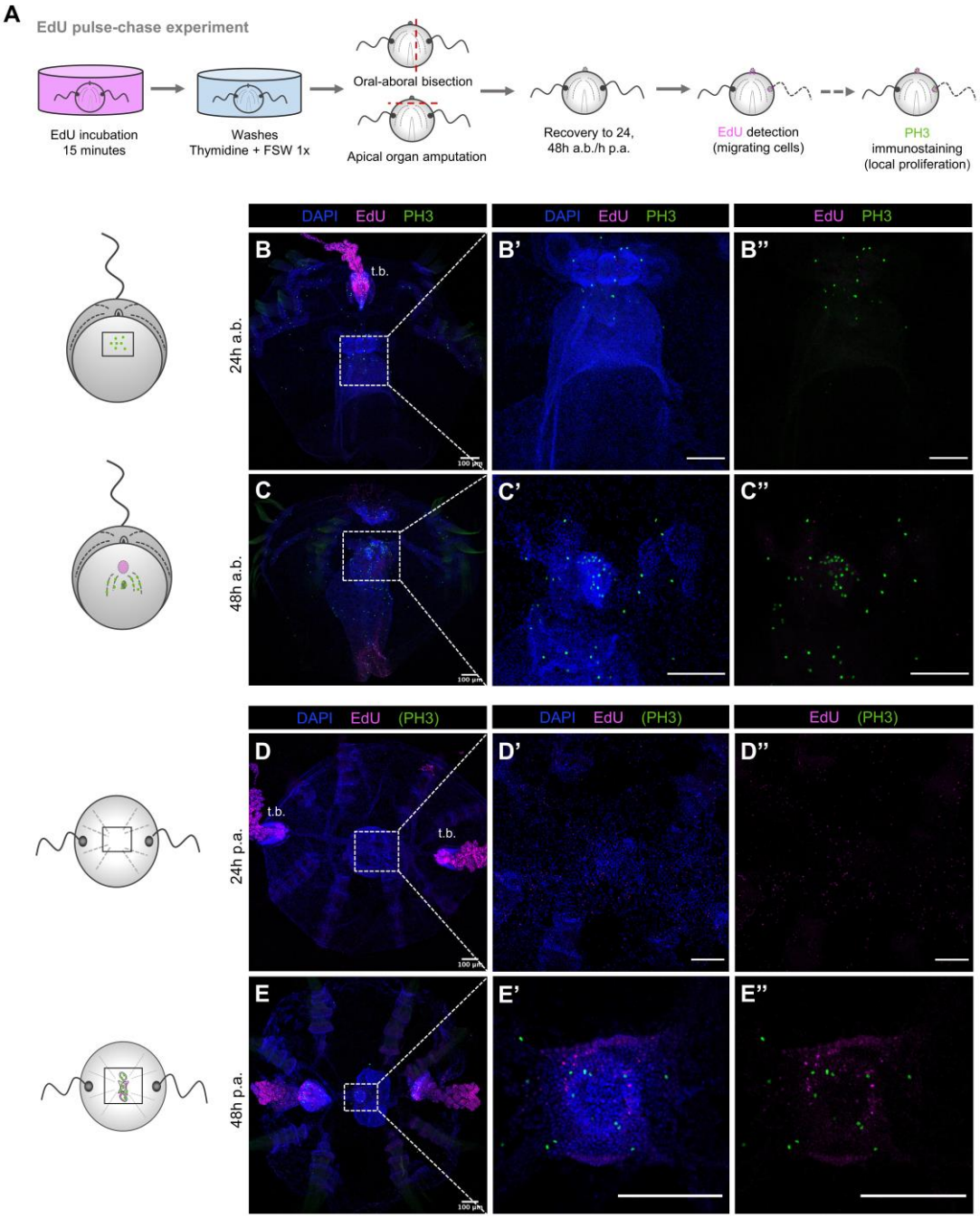

Figure 8. S-phase cells derived from the main regions of cell proliferation do not contribute to the formation of new structures. (**A**) Schematic of the EdU pulse-chase experiments and PH3 immunostaining in regenerating cydippids after oral-aboral bisection and apical organ amputation. (**B-C''**) Confocal stack projections of bisected cydippids through the oral-aboral axis oriented in a lateral view showing the cut site in the first plane. (**D-E''**) Confocal stack projections of cydippids in which the apical organ was amputated oriented in an aboral view. The labeling corresponding to each panel is listed at the top of the columns, and the time of chase is listed to the left of the rows. Nuclei of S-phase cells are labeled with EdU (magenta), M-phase cells are stained with anti-PH3 (green) and all nuclei are counterstained with DAPI (blue). Dotted line rectangles in (**B**), (**C**), (**D**) and (**E**) show the area corresponding to higher magnifications on the right. The pattern of EdU and PH3 staining is shown in cartoons on the left. Scale bars = 100 μm. Abbreviations: tentacle bulb (t.b.), hours after bisection (h a.b.), hours post amputation (h p.a.).

Figure 9

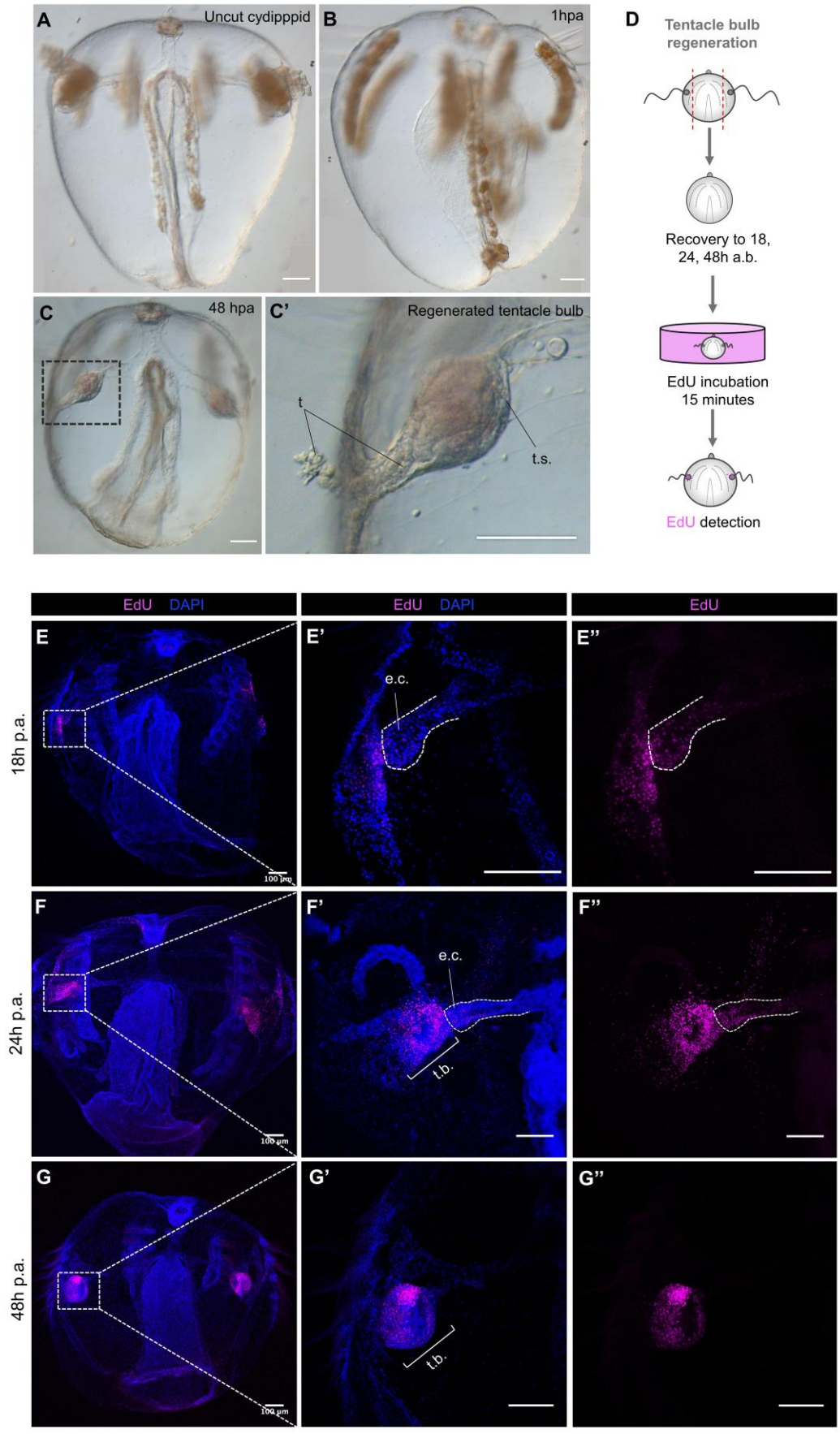

Figure 9. Regeneration occurs after removal of the main regions of active cell proliferation. (**A-C'**) DIC images of an uncut cydippid (**A**) and cydippids after tentacle bulbs amputation (**B-C'**). Black dotted line rectangle in (**C**) show the area corresponding to higher magnification on the right. (**D**) Schematic of the EdU incorporation experiment in cydippids in which both tentacle bulbs were amputated. (**E-G''**) Confocal stack projections of cydippids in which the tentacle bulbs were amputated oriented in a lateral view at different time points post amputation. The labeling corresponding to each panel is listed at the top of the columns, and the time following amputation is listed to the left of the rows. Dotted line rectangles in (**E**), (**F**) and (**G**) show the area corresponding to higher magnifications on the right. Nuclei of S-phase cells are labeled with EdU (magenta) and all nuclei are counterstained with DAPI (blue). Scale bars = 100μm. Abbreviations: tentacle sheath (t.s.), tentacle (t), endodermal canal (e.c.), tentacle bulb (t.b.), hours after bisection (h a.b.), hours post amputation (h p.a.).

Figure 10

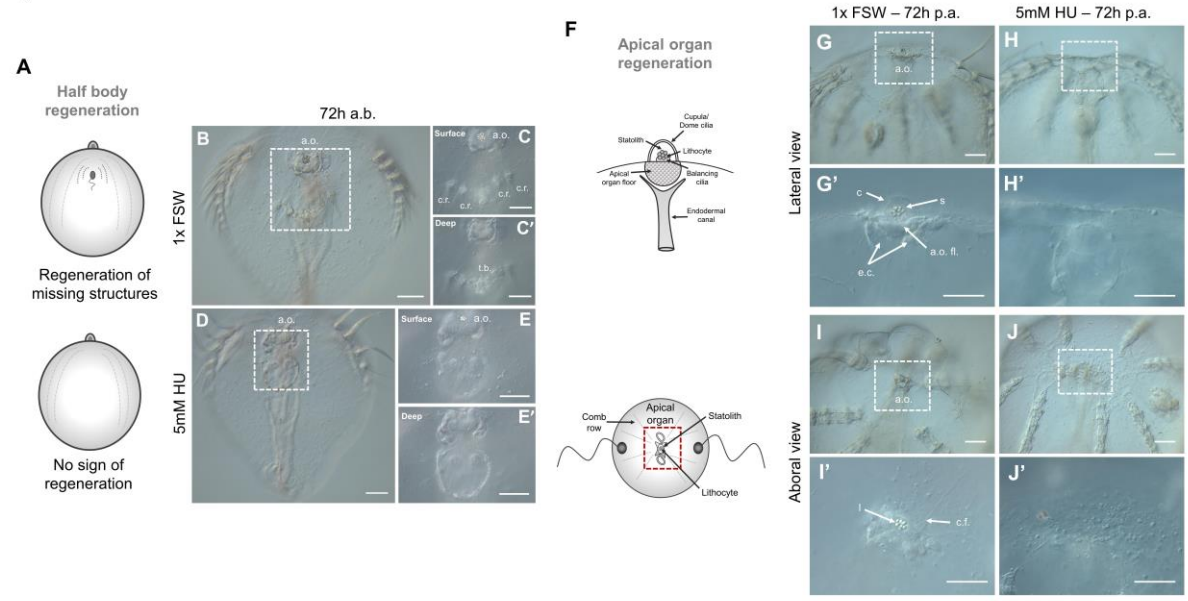

Figure 10. Ctenophore regeneration does not occur in the absence of cell proliferation. (**A**) Schematic representation of the regeneration state of cydippids shown in the panels on the right. Cartoons correspond to lateral views of the cydippid's body bisected in half through the oral-aboral axis showing the cut site in the first plane. (**B-E'**) DIC images of bisected cydippids in a lateral view at 72 hab. The type of treatment corresponding to each panel is listed to the left of the rows. Dotted line rectangles in (**B**) and (**D**) show the area corresponding to higher magnifications on the right. Magnifications show surface (top) and deep (bottom) planes. Note that the wound site in treated cydippids is covered by a continuous epithelium but there is no sign of formation of missing structures. (**F**) Schematic representation of the apical sensory organ in lateral (top) and aboral (bottom) views. Red dotted rectangle at the bottom cartoon delimits the apical organ area shown in the images on the right. (**G-H'**) DIC images of cydippids in which the apical organ was amputated at 72 hpa orientated in a lateral view. (**I-J'**) DIC images of cydippids in which the apical organ was amputated at 72 hpa orientated in an aboral view. The type of treatment corresponding to each panel is listed to the top of the columns. Dotted line rectangles in (**G**), (**H**), (**I**) and (**J**) show the area corresponding to higher magnifications on the bottom. Note that treated cydippids show aggregation of cells around the surface of the wounded area although none of the missing apical organ structures are formed. Scale bars = 100 μm. Abbreviations: hours after bisection (h a.b.), hours post amputation (h p.a.), apical organ (a.o.), comb row (c.r.), tentacle bulb (t.b.), statolith (s), cupula (c), apical organ floor (a.o. fl.), endodermal canal (e.c.), lithocyte (l), ciliated furrow (c.f.).

Figure 11

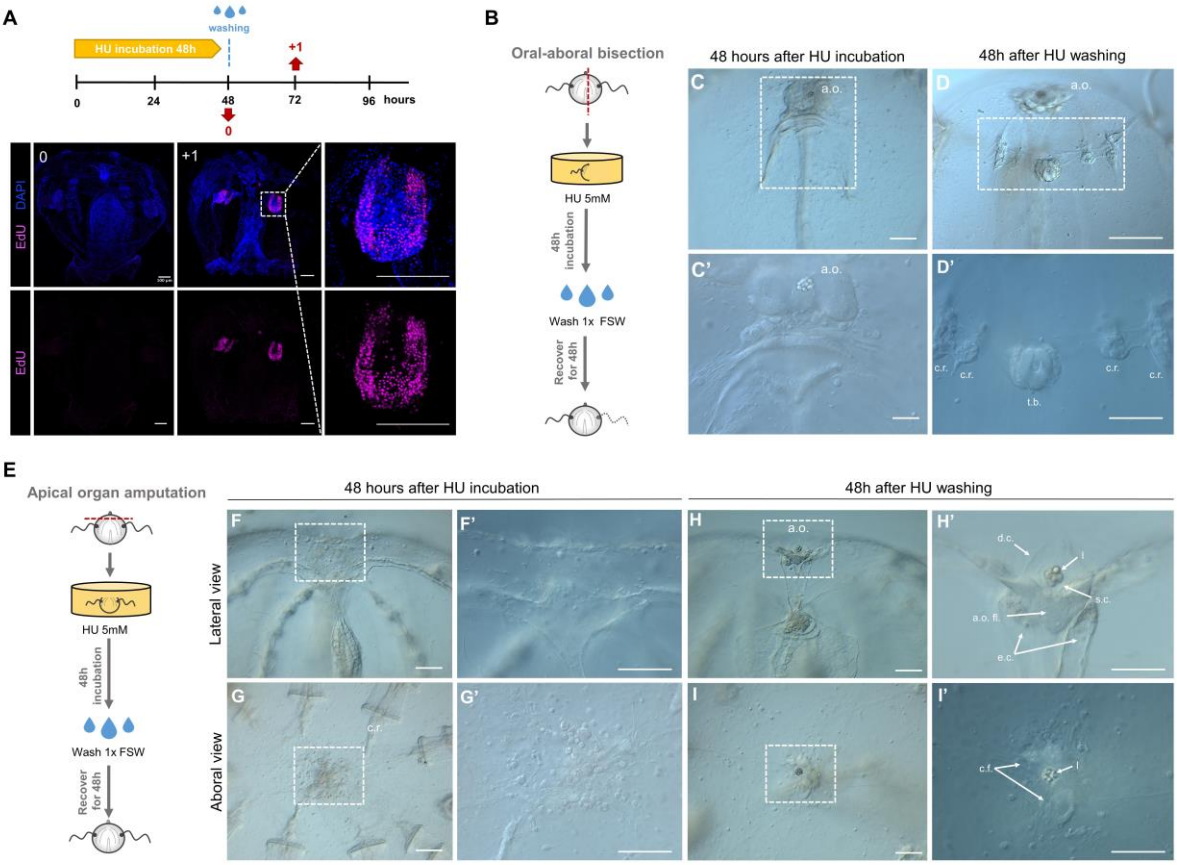

Figure 11. Regenerative ability is recovered after HU treatment ends. (**A**) Reversible S-phase arrest after HU treatment as detected by EdU labeling performed at the indicated time-points (red arrows). Nuclei of S-phase cells are labeled with EdU (magenta) and all nuclei are counterstained with DAPI (blue). Note that cells have already resumed cell cycle progression 1 day after HU wash (**B**) Schematic representation of HU treatment and wash experiment in bisected cydippids through the oral-aboral axis. (**C-C'**) DIC images of bisected cydippids in lateral view showing the wound site at 48 hab (just after HU treatment and before washing). The dotted line rectangle in (**C**) shows the area corresponding to higher magnification at the bottom. Note that there is no sign of regeneration of the missing structures. (**D-D''**) DIC images of bisected cydippids in lateral view showing the wound site at 96 hab (48h after HU wash). The dotted line rectangle in (**D**) shows the area corresponding to higher magnification at the bottom. Note that all missing structures (comb rows and tentacle bulb) are regenerated. (**E**) Schematic representation of HU treatment and wash experiment in cydippids in which the apical organ was amputated. (**F-G'**) DIC images of amputated cydippids oriented in a lateral (top panels) and aboral (bottom panels) view showing the wound site at 48 hpa (just after HU treatment and before washing). Dotted line rectangles in (**F**) and (**G**) shows the area corresponding to higher magnification on the right. Note that there is no sign of regeneration of the missing structures. (**H-I'**) DIC images of amputated cydippids oriented in a lateral (top panels) and aboral (bottom panels) view showing the wound site at 96 hpa (48h after HU wash). Dotted line rectangles in (**H**) and (**I**) show the area corresponding to higher magnification on the right. Note that all components of the apical organ are regenerated. Scale bars = 100 μm. Abbreviations: hours after bisection (h a.b.), hours post amputation (h p.a.), apical organ (a.o.), comb row (c.r.), tentacle bulb (t.b.), dome cilia (d.c.), lithocyte (l), supporting cilia (s.c.), apical organ floor (a.o. fl.), endodermal canal (e.c.), ciliated furrows (c.f.).

Figure 12

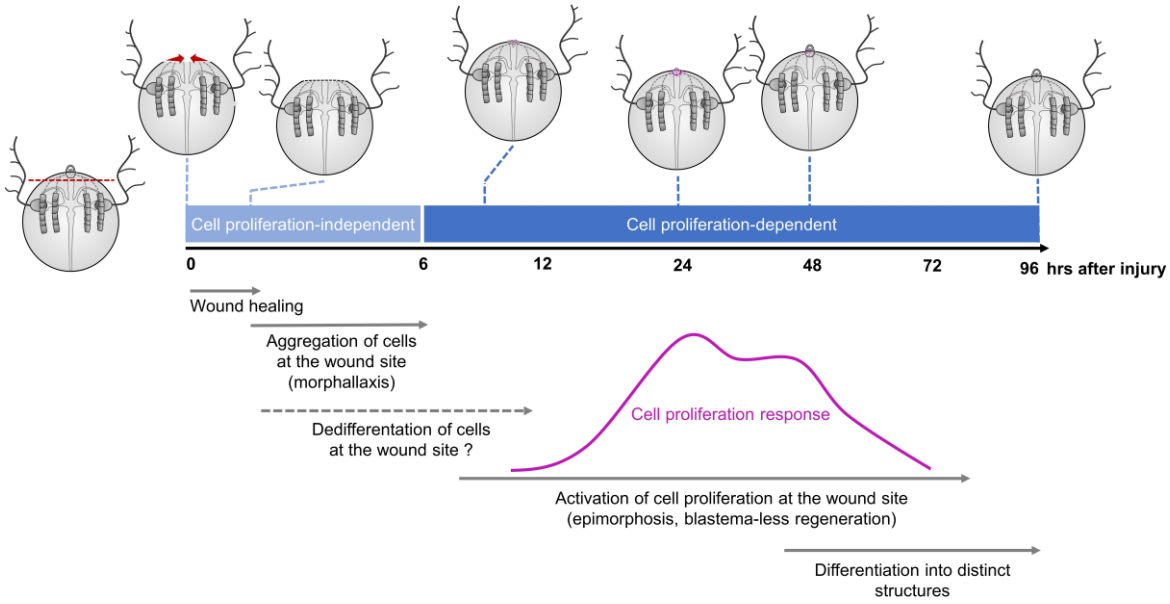

Figure 12. Working model of ctenophore regeneration. Timeline of the morphological and cellular events underlying ctenophore regeneration. Apical organ regeneration is used as example. Proliferating cells (EdU+) are colored in magenta. Wound closure is initiated immediately after surgery with the edges of the wound forming a round circumference that reduces in diameter until meeting and is completed within 1-2 hours after amputation. Reorganization of tissue including aggregation of round-shaped cells at the wound epithelium – potentially derived from dedifferentiation – events takes place during the first 6 hours after injury (Cell-proliferation independent phase). Cell proliferation is activated at the wound site between 6-12 hours after amputation and it reaches a maximum at 24 hours, when the primordia of the missing structures are formed. After this peak of cell proliferation, the number of proliferating cells at the wound site decreases while cells start to specify and differentiate into the final structures.